



# Eco-toxicological and climate change effects of sludge thermal treatments: Pathways towards zero pollution and negative emissions

Marjorie Morales<sup>a,\*</sup>, Hans Peter H. Arp<sup>b,c</sup>, Gabriela Castro<sup>b,d</sup>, Alexandros G. Asimakopoulos<sup>b</sup>, Erlend Sørmo<sup>c,e</sup>, Gregory Peters<sup>f</sup>, Francesco Cherubini<sup>a</sup>

<sup>a</sup> Industrial Ecology Programme (IndEcol), Department of Energy and Process Engineering, Norwegian University of Science and Technology (NTNU), 7034 Trondheim, Norway

<sup>b</sup> Department of Chemistry, Norwegian University of Science and Technology (NTNU), 7491 Trondheim, Norway

<sup>c</sup> Norwegian Geotechnical Institute (NGI), 0886 Oslo, Norway

<sup>d</sup> Department of Analytical Chemistry, Nutrition and Food Sciences, Institute for Research in Chemical and Biological Analysis (IAQBUS), Universidade de Santiago de Compostela, 15782 Santiago de Compostela, Spain

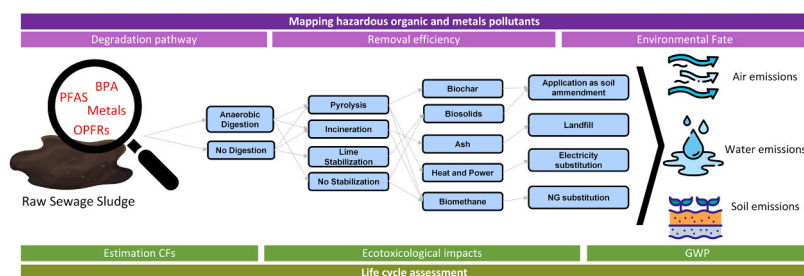
<sup>e</sup> Norwegian University of Life Sciences (NMBU), 1430 Ås, Norway

<sup>f</sup> Division of Environmental Systems Analysis, Chalmers University of Technology, Gothenburg, SE 412 96, Sweden

## HIGHLIGHTS

- A wide range of novel characterization factors for PFAS and OPFRs are estimated.
- Pyrolysis and incineration degrade from 94 % to 99 % of PFAS, OPFRs and BPA.
- HMs are the dominant pollutants affecting human health and freshwater ecotoxicity.
- Direct pyrolysis is the best option to deliver negative emissions and abate HOCs.
- Conventional treatments leave about 40 % of OPFRs unabated, and no PFAS degradation.

## GRAPHICAL ABSTRACT



## ARTICLE INFO

### Keywords:

Wastewater treatment  
Heavy metals  
Anaerobic digestion  
PFAS

## ABSTRACT

The high moisture content and the potential presence of hazardous organic compounds (HOCs) and metals (HMs) in sewage sludge (SS) pose technical and regulatory challenges for its circular economy valorisation. Thermal treatments are expected to reduce the volume of SS while producing energy and eliminating HOCs. In this study, we integrate quantitative analysis of SS concentration of 12 HMs and 61 HOCs, including organophosphate flame retardants (OPFRs) and per- and poly-fluoroalkyl substances (PFAS), with life-cycle assessment to estimate

**Abbreviations:** AD, anaerobic digestion; CFs, characterization factors; CHP, combined heat and power; C1-C6, scenarios considered for sludge management; EF, effect factor; FF, fate factor;  $f_{oc}$ , organic carbon fraction;  $f_s$ , fraction sorbed in solid phase at equilibrium; FTS, fluorotelomer sulfonate compounds; GTP100, 100-years Global Temperature Potential; GWP20, 20-years Global Warming Potential; GWP100, 100-years Global Warming Potential; HMs, hazardous metals; HOCs, hazardous organic compounds;  $K_d$ , solid-water partition coefficient;  $K_{OC}$ , organic carbon content-normalized partition coefficient; LCA, life cycle assessment; LOD, limit of detection; OPFRs, organophosphate flame retardants; PAF, potentially affected fraction of aquatic species; PFAS, per- and poly-fluoroalkyl substances; PFCA, perfluoroalkyl carboxylates; PFSA, perfluoroalkane sulfonates; PreFOS, perfluorooctane sulfonate precursors; SLCPs, short-lived climate pollutants; SS, sewage sludge; WWTPs, wastewater treatment plants; WMGHGs, well-mixed greenhouse gases; XF, exposure factor.

\* Corresponding author.

E-mail address: [marjorie.morales@ntnu.no](mailto:marjorie.morales@ntnu.no) (M. Morales).

<https://doi.org/10.1016/j.jhazmat.2024.134242>

Received 16 November 2023; Received in revised form 21 February 2024; Accepted 7 April 2024

Available online 10 April 2024

0304-3894/© 2024 The Authors. Published by Elsevier B.V. This is an open access article under the CC BY license (<http://creativecommons.org/licenses/by/4.0/>).

Pyrolysis  
OPFRs

removal efficiency of pollutants, climate change mitigation benefits and toxicological effects of existing and alternative SS treatments (involving pyrolysis, incineration, and/or anaerobic digestion). Conventional SS treatment leaves between 24 % and 40 % of OPFRs unabated, while almost no degradation occurs for PFAS. Thermal treatments can degrade more than 93% of target OPFRs and 95 % of target PFAS (with the rest released to effluents). The different treatments affect how HMs are emitted across environmental compartments. Conventional treatments also show higher climate change impacts than thermal treatments. Overall, thermal treatments can effectively reduce the HOCs emitted to the environment while delivering negative emissions (from about -56 to -111 kg CO<sub>2</sub>-eq per tonne of sludge, when pyrolysis is involved) and producing renewable energy from heat integration and valorization.

## 1. Introduction

The production of sewage sludge (SS) has dramatically increased worldwide over the last two decades as a result of increasing population and living standards [21]. In Europe, the sludge production based on the most recent supported statistics in 2021 is around 5.5 million tonnes of dry solids per year [25]. Although the volume of SS produced is only 2 % of the initial wastewater volume, its treatment and disposal account for up to 50 % of the total operational and capital costs of wastewater treatment plants [21].

Incineration of dried sludge and landfilling remain the primary sludge disposal practices in most of the countries [15], but environmental policies tend to tighten environmental regulations and reduce landfill disposals to incentivize solutions for recycling [46]. Sludge can be used as a soil amendment in agriculture [2] or as a source of heat in industrial applications (e.g., cement production) [14]. The main re-use route in the EU is application to agricultural soils (45 % directly and 7 % after composting) [47]. In Norway, total sludge production showed an average annual growth of 6 % in the last few years, reaching 134,000 tonnes of dry solids in 2021 [81], and around 79% of SS is used in agriculture, green spaces as parks, or delivered to fertilizer producers [80].

Although applications in agriculture and in green areas make use of some nutrients contained in the sludge, they also risk releasing toxic pollutants into the environment [8]. The sludge is a collector sink of hazardous organic compounds (HOCs), hazardous metals (HMs), pharmaceutical products, pesticides, and microplastics, among others, at various concentrations [55]. Among the HOCs, per- and polyfluoroalkyl substances (PFAS), a complex group of synthetic chemicals that have been used in consumer products since the 1950 s, and organophosphate flame retardant (OPFRs), a group of chemicals used as flame retardants and plasticizers, are of rising concern because of their long-lasting persistence in the environment and food products, with increasing studies showing that exposure to these HOCs is linked to harmful health effects in humans and animals [5,67]. HMs have been reported to affect biochemical and physiological functions in plants and animals, and induce adverse health effects in humans, such as neurologic, cardiovascular and developmental diseases, and various types of cancer [11, 31].

The EU is considering reducing the limits of the contamination levels allowed in SS used as fertilizer, with some countries already adopting lower levels [40]. Stricter limits will increase costs and reduce the contamination levels for potential applications [24]. There is an urgent need for improved and efficient management solutions for sludge that can safely stabilize, remove or reduce its content of pollutants [28].

Thermal treatments such as anaerobic digestion, pyrolysis, hydrothermal processes, and incineration are options for reducing the waste to be landfilled, while allowing waste hygienization and energy recovery. Thermal treatments can convert the sludge into energy directly [63] or by producing a gas rich in CH<sub>4</sub> and/or H<sub>2</sub>, which can in turn be used as an energy carrier [30]. Currently, anaerobic digestion is frequently applied to SS and the resulting digestate is used in agriculture. This technology recovers about 50 % of the organic matter by producing biogas but only partly addresses the issue of degradation of pollutants

[42]. Thermal treatment of SS via incineration in EU has increased [44]. Incineration has the advantage to recover useful energy and destroy several toxic organic contaminants contained in the sludge (though not HMs). However, it does not valorize nutrient and material contents of SS and might increase risks of air pollution. Pyrolysis of SS is still at a pre-commercial scale, but its use, either stand-alone or integrated with anaerobic digestion, is gaining rapid interest as a solution to maximize energy and material outputs (e.g., in the form of biochar) while safely degrading most of the toxic contaminants [70].

Despite the importance of the topic and the need to optimize management strategies from a sustainability perspective, there is limited information on the environmental trade-offs of implementing these technologies and, even more, on the efficiency by which they can remove toxic pollutants. Some existing studies based on Life-Cycle Assessment (LCA) of sludge treatment via pyrolysis [27,32,39], hydrothermal treatment [54,59] or incineration [27,58] mainly focus on climate change effects and/or rely on hypothetical systems and process simulation as data source. When human toxicity or freshwater ecotoxicity impacts are considered [27,32,39], they mostly rely on simplified and generic factors without considering the main sources of these impacts and/or tracking the fate of the individual contaminants and their release to the environment through the different treatment stages. An accurate mapping of the fate of the various pollutants from measuring their levels in real samples collected before and after each treatment stage can inform about the effectiveness of abatement of each treatment method. Further, while toxicity impact factors are available for most HMs, this is not the case for most HOCs, preventing an accurate estimate of their effects on human and ecosystem health once released to different environmental compartments (air, freshwater, soil, etc.). Despite the large number (more than 3000) of substances included in the USEtox™ database, the most common source for toxicity impact factors in LCA, data are available for only twelve OPFRs and very few PFAS (e.g., PFOA, PFHxA, PFBS) [36].

In this study, we integrate laboratory measurements of contaminants concentration in 32 samples (14 sampling campaigns) of sewage sludge collected before and after thermal treatments at running wastewater treatment plants (WWTPs) and at a pyrolysis pilot plant in Norway with an LCA approach where alternative treatment scenarios are compared in terms of climate change mitigation benefits, removal efficiency of hazardous substances (PFAS, OPFRs, and HMs), and toxicity impacts. The scenarios are based on individual (or combinations of) thermal/non-thermal treatments such as anaerobic digestion, de-watering, stabilization, drying, pyrolysis, incineration, and valorisation of co-products (biogas upgrading, heat and power cogeneration, biochar application to soils). Process simulation is used to compute an accurate mass and energy balance of each treatment scenario, and novel characterization factors to estimate the toxic impacts of emissions to air, water, and soils of a variety of PFAS and OPFRs are calculated and applied. Different climate metrics and a Monte-Carlo uncertainty analysis are applied to explore variability in the results from a large variety of process factors and model uncertainties. Results are presented as statistical outcomes from 10,000 repetitions of the analysis by randomly selecting any possible value within the given uncertainty ranges of each uncertainty factor.

## 2. Materials and methods

Fig. 1 shows an overview of the methods and data used to map the fate of HMs and HOCs throughout the treatment scenarios and estimate the corresponding life-cycle environmental impacts. The first step consisted of sampling and analyzing the concentrations of HOCs and HMs in raw SS from 6 Norwegian WWTPs, which provided the composition of the input materials and concentration profiles of the pollutants (Section 2.1). This information was fed into Aspen Plus in Step 2 to quantify the mass and energy flows at the level of unit process for the identified SS management options, as described in Section 2.2. The third step involved a combination of documented literature and laboratory data to quantify the removal efficiency of pollutants at each process stage of SS treatment and map the fate of HOCs and HMs within each process unit and their release to water, air or soil (Section 2.3). In the fourth step, the eco-toxicity characterization factors for a variety of HOCs (mostly PFAS) were determined using up-to-date environmental impact assessment models based on stressor-response mechanisms, exposure risks, and health effects (Section 2.4). The fifth step involved the characterization of the climate change and toxicity impacts (LCA results) for the SS treatment scenarios considered in this study (section 2.5).

### 2.1. Sample collection and types of contaminants

Raw SS samples were obtained from five wastewater treatment plants (WWTP-1, WWTP-2, WWTP-3, WWTP-4, and WWTP-5) and one sludge treatment plant (STP-6) located in the Trondelag, Viken and Oslo regions. The WWTP-1 and WWTP-2 are serving the city area of Trondheim (Central Norway), and they are designed for a capacity of 170,000 PE (Population Equivalent) and 120,00 PE, respectively, with a disposed sludge of 1799 tonnes TS-year<sup>-1</sup> and 1750 tonnes TS-year<sup>-1</sup> (where TS means Total solids, based on dry sludge). The largest unit (WWTP-3) is serving the Metropolitan area of Oslo (750,000 PE), with 16,966 tonnes TS-year<sup>-1</sup> of SS. The other plants are situated in the Viken Region (South-East Norway), in Moss, Gardermoen and Drammen, respectively. WWTP-4 and WWTP-5 serve approximately 80,000 PE, and the disposed sludge is 683 and 1185 tonnes TS-year<sup>-1</sup>, respectively. STP-6 receives

sludge from various treatment plants, treating 3310 tonnes TS-year<sup>-1</sup>, and it converts sludge into biogas through thermal hydrolysis and mesophilic anaerobic stabilization.

The samples were collected in different seasons during 2020 and 2021 after primary (WWTP-1 to 5) and activated sludge treatment (STP-6) (sampling description in Castro et al. [13] and Castro et al. [12]). The samples of raw sludge in WWTPs have been taken before treatment such as digestion or lime application to avoid effects on the concentration of organic pollutants, and after digestion. Samples of wastewater and raw sludge were taken in 1-L amber glass jars or 1-L HDPE jars; in the case of digested sludge, 10 kg of sample was collected in sterile polypropylene bags. Once in the laboratory, samples of wastewater were filtered through a glass microfiber filters GF/F diameter 47 mm (WhatmanTM, VWR, Norway), previously baked to reach 0.45 µm pore size, and sludge was frozen at -20 °C in aluminum foil containers for 12 h and freeze-dried (-21 °C, 6 mbar). Dried samples were homogenized in a mortar and kept at 4 °C until analysis. Extraction and analysis of OPFRs, BPA and PFAS was performed according to previous work with minor modifications [12,13,43,83]. Target chemical quantification was accomplished using internal standards and matrix-matched calibration curves prepared by spiking the target chemicals and internal standards into the matrix prior to extraction modifications. Details about extraction and analysis are available in the Supplementary Text 1 and Tables S1-3 in Appendix A.

Twelve HMs were detected and analyzed in the raw SS: arsenic (As), barium (Ba), cadmium (Cd), cobalt (Co), chromium (Cr), copper (Cu), molybdenum (Mo), nickel (Ni), lead (Pb), strontium (Sr), vanadium (V) and zinc (Zn). The targeted HOCs include 21 OPFRs, 39 PFAS and 1 bisphenol (bisphenol A [BPA]). These HOCs were selected due to increasing interest by policy makers, their high persistence and toxicity, particularly regarding food safety [22,23,51]. Regarding the OPFRs, four chlorinated, seven aryl and ten alkyl compounds were detected in the sludge. The PFAS include four fluorotelomer sulfonate compounds (FTS), fifteen perfluoroalkyl carboxylates (PFCA), nine perfluoroalkane sulfonates (PFSA), seven perfluorooctane sulfonate precursors (PreFOS) and four uncategorized compounds. The full list of HOCs and HMs considered in this study is available in Table S4. The laboratory analysis

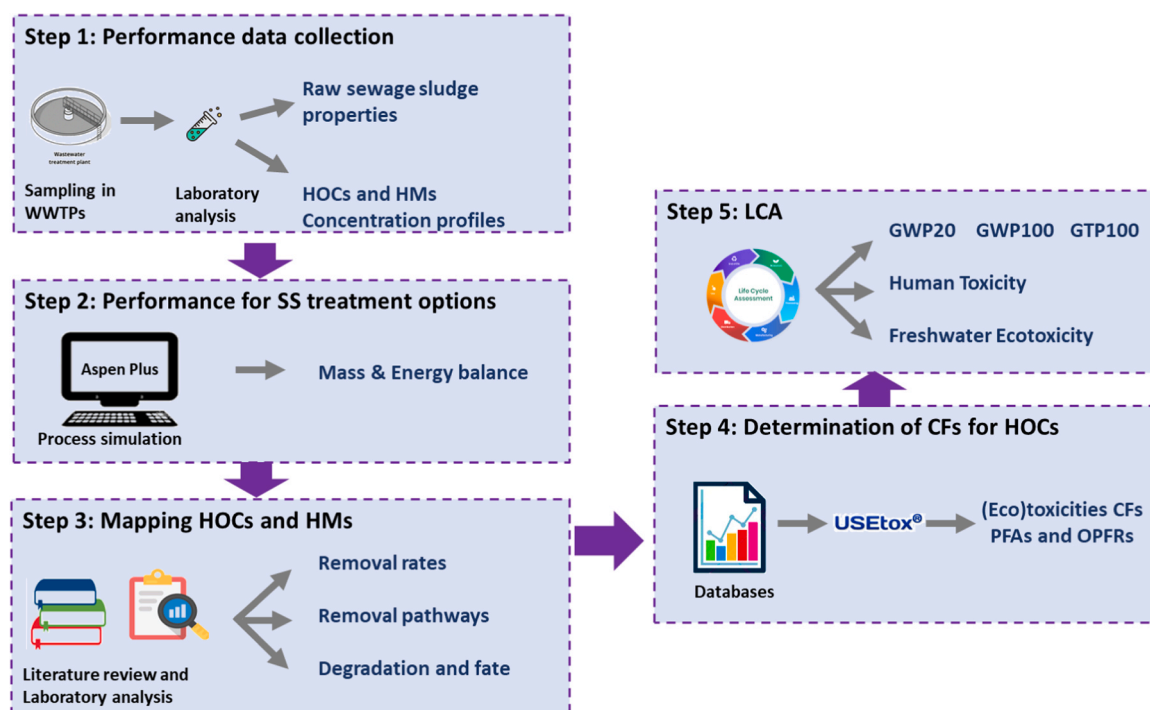


Fig. 1. Main steps of the methodological framework used in this study.

finds that OPFRs are the HOC that are most abundantly detected in the raw SS in Norway (the average of all OPFRs is  $2023.2 \pm 1564.5$  ng/g-dwSS, where dwSS means dry weight sewage sludge), followed by PFAS (average:  $560.3 \pm 47.28$  ng/g-dwSS) and BPA ( $50.1 \pm 39.6$  ng/g-dwSS). The highest concentration of PFAS were observed for the PFAS-PFCA (78.7 % of all PFAS), while PFAS-PreFOS, PFAS-PFSA, PFAS-FTS and PFAS-uncategorized represent 10.6 %, 8.9 %, 1.12 % and 0.66 %, respectively. The concentration in raw (pre-digested) SS of each HOC and HM, together with other types of information such as proximate and ultimate analysis, is reported in Table S5.

One of the scenarios of SS treatment includes pyrolysis. As a commercial pyrolysis plant is not available yet, data are taken from samples of SS and resulting biochar and emissions to air from a pilot plant. This plant consists of a medium scale ( $2 - 10$  kg·h<sup>-1</sup>) Biogreen© pyrolysis unit (ETIA, France), which was installed by VOW ASA (Lysaker, Norway). The pyrolyzer consists of an electrically heated reactor (up to 800 °C), a condenser unit for pyrolysis gas ( $\approx 10$  °C) with a collection tray for the pyrolysis oil, and a combustion chamber (700–900 °C) for the remaining pyrolysis gas [83]. The resulting biochar, produced at different temperatures (500–800 °C) during a 2-hr period of stable conditions at a given pyrolysis temperature ( $\sim 4-10$  kg produced in total), was subsampled (100 g) and stored in glass jars (200 mL). Pyrolysis samples are grouped at 550 °C (those ranging from 500 °C to 600 °C) and 750 °C (from 700 °C to 800 °C). Before pyrolysis, the digested sludge was submitted to drying in batches of 2 m<sup>3</sup> of sewage sludge (5–10% moisture) in a paddle dryer (1.5 × 5 m) operating at 102–110 °C. Water was removed at a rate of 300 L hour<sup>-1</sup> by a superheated steam, supplied from a heat exchanger into a heating jacket fitted around the drier. Dried samples were then pelletized (length 40 mm,

radius 8 mm) before pyrolysis [13,83]. Pyrolysis gas composition was measured by Fourier Transform Infrared Spectrometer (FTIR, Gaset) and aerosols (PM10) with a pdr-1500 (Thermo Scientific). Emission factors for gases and contaminants were calculated using the carbon balance approach as described by Sørmo et al. [83].

### 2.2. Alternative scenarios for sludge management

Eight different scenarios for sludge management were considered (Fig. 2). The first is a baseline case (C1) that represents a common treatment that includes lime stabilization and de-watering to produce bio-solids (or de-watered sludge) to be disposed as fertilizer on land areas. The second baseline case (C2) includes anaerobic digestion instead of lime stabilization, followed by dewatering and upgrading of biogas to produce methane and replace natural gas. Both C1 and C2 are representative of current options of SS treatment in Norway and are used to benchmark the environmental performances of six alternative scenarios that include thermal treatments (pyrolysis and incineration), with or without anaerobic digestion (AD). Pyrolysis is the thermal treatment considered in C3, where SS initially undergoes AD and then the digested sludge is pyrolyzed, and C4, where AD does not occur. The pyrolysis cases were evaluated at both low (500–600 °C, averaged results indicated as 550 °C) and high (700–800 °C, averaged results indicated as 750 °C) temperatures, with energy recovery via combined heat and power (CHP) from bio-oil and pyrolysis gas in a boiler and use of biochar in agriculture. The energy produced (heat and power) is partially used to meet the internal energy demand of the treatment plants, and the rest is exported to the energy market (as power, heat only produced for internal use). In C5 and C6, SS is sent to incineration (850 °C, 0.3 MPa) either directly after de-watering and drying (C6) or after AD, de-

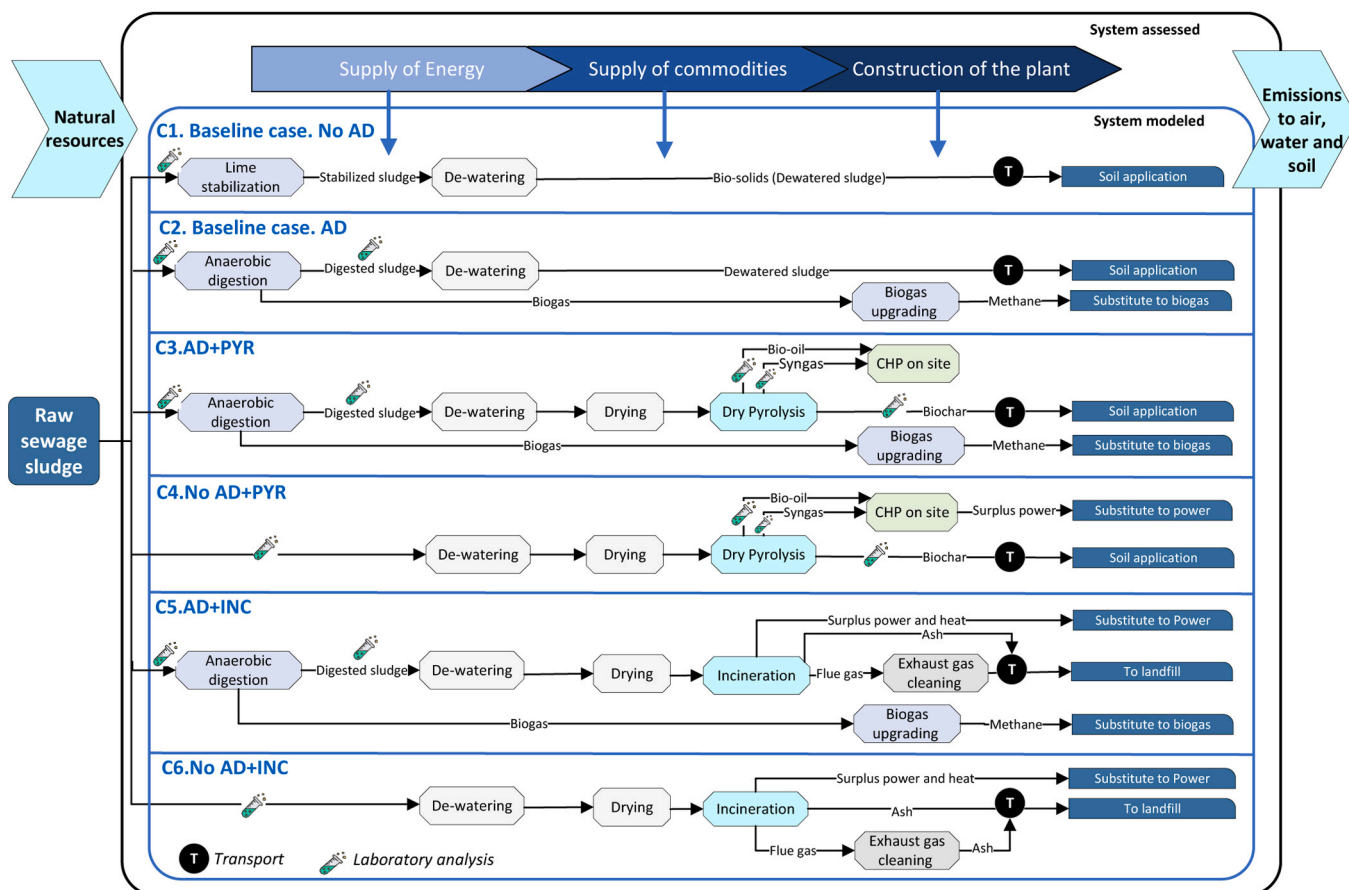


Fig. 2. Overview of the alternative scenarios of sludge treatment, with their main steps and system boundaries. The scheme also indicates the process steps/flows for which laboratory analysis are performed.

watering and drying (C5) and ash disposal to a landfill. In both cases, heat and power are produced from energy recovery and partially used to meet the internal energy demand, while the surplus is exported to the energy market (as electricity).

The main process stages of SS treatment scenarios (sludge stabilization, de-watering, drying, AD, biogas upgrading, pyrolysis, and incineration) and modelling of their technological parameters are explained in detail in Supplementary Text 2, while the individual scenarios and their configurations are described in Supplementary Text 3. The process modelling was built using experimental laboratory data and complemented by bibliographic information in Aspen Plus v10.1 process simulation software. Conventional and nonconventional components were defined. Nonconventional refers to heterogenous components that do not participate in chemical or phase equilibrium, with enthalpy and density being the only properties defined. These nonconventional components include the feedstock biomass (contained in raw SS), biochar, bio-oil and ash. Process modelling uses HCOALGEN and DCOALIGT as property models to calculate the enthalpy and density for the nonconventional compounds by providing the proximate, ultimate and sulfanal data analysis. The proximate and ultimate analysis of biochar and bio-oil based on laboratory data from the analysis of samples from the pilot plant (complemented with literature data and/or simulations when needed) are available in Table S12, and those for pyrolysis gas in Table S10 (bio-oil and pyrolysis gas sent to CHP unit to produce energy). The inventory data containing all inputs and process outputs of each investigated scenario is available in Table S13, and the gaseous emission compositions from CHP boiler and incinerator in Table S14.

### 2.3. Removal rates of HOCs and HMs

Available information on the fate and transformation of contaminants during the various treatments of SS is limited [35]. The existing studies mostly focus on conventional treatments and rely on individual (point) measurements or assumptions from process simulations. In this study, we rely on extensive measurements and laboratory analysis before and after the main process stages, i.e., AD and pyrolysis, to estimate the removal rates and speciation data for HOCs and HMs. Information on the speciation and degradation from lime stabilization, de-watering, drying and incineration are collected from the literature (data source are listed in Table S15 and removal rates in Table S16). The main removal rates and degradation processes in each stage for OPFRs, PFAS, BPA and HMs are described in the following subsections.

#### 2.3.1. Lime stabilization

During lime stabilization, the pH of the sludge increases, which reduces the solubility, mobility, and toxicity of various HOCs and HMs in SS. The removal rates for 15 OPFRs in the expected basic solution after lime addition (pH = 11–13) are taken from the literature [82], while removal efficiency for 6 OPFRs (TiBP, DPMP, BBOEHEP, 3OH-TBOEP, RDP and BPA-BDPP) are based on structural similarity with other OPFR for which data are available. For example, a 10 % removal for TiBP is considered, in line with TnBP. Base-catalyzed hydrolysis of the phosphate ester bond of OPFRs (OP triesters to OP diesters as end products) is the most relevant mechanism of degradation [82]. The pH-value affects desorption of BPA from solid to liquid phase, and a pH around 12 induces a 92% desorption, which corresponds to  $pK_a = 10.3$  for BPA [41]. Similar to BPA, pH-values affect the mobility of PFAS. PFAS tends to attach to solid phase, and alkaline environments reduce the potential leachability of PFAS and increase the sorption to sludge solid phase. PFAS compounds are strong acids, having  $pK_a$  values less than 1.6 [88]. For simplicity, it is assumed that PFAS at pH= 12 are immobilized as calcium salts that are immobilized in the sludge [53], with a 0 % desorption to the liquid phase after lime stabilization. For HMs, the pH changes their leaching behavior, affecting the fractionation and extractability [38]. As the lime stabilization is proceeding, certain metals are transported into the aqueous phase [76]. The HM extraction

rates for Ar, Cd, Cr, Cu, Ni, Pb and Zn (% removal) after lime stabilization are obtained from the literature [38,76], while for the remaining HMs (Ba, Co, Mo, Sr, V) it is assumed to be an average value based on the reported factors for the other metals (24.5 % ± 19.3).

#### 2.3.2. De-watering

The partition coefficient  $K_d$  is often used to characterize the affinity of organic substances to the aqueous or solid phase, [41]. The greater this coefficient is, the higher is the affinity to solid phase. The partition coefficient  $K_d$  (in L/kg) is defined as Arvaniti et al. [6]:

$$K_d = \frac{C_s}{C_w} \quad (1)$$

where  $C_s$  is equilibrium HOCs concentration in the sludge ( $\mu\text{g}/\text{kg}$ ) and  $C_w$  is the equilibrium HOCs concentration in the liquid phase ( $\mu\text{g}/\text{L}$ ). The fraction ( $f_s$ ) of each target compound that would be sorbed in solid phase at equilibrium for a given sludge concentration (suspended solids, SS, in  $\text{kg}/\text{L}$ ) is defined as Eq. 2 [6]:

$$f_s = \frac{SS \cdot K_d}{1 + (SS \cdot K_d)} \quad (2)$$

The removal efficiency,  $Removal_i(\%)$ , indicating the discharge of component  $i$  along with the effluents (de-watered compound), is calculated as:

$$Removal_{i,de-watering} = (1 - f_s) \cdot 100 \quad (3)$$

Data of  $K_d$  of all the HOCs are reported in Table S17. For 8 OPFRs, data were obtained from the literature [51] and their average log  $K_d$  ( $2.79 \pm 0.71$ ) is used as a proxy for the missing  $K_d$  values of the other OPFRs. For BPA, log  $K_d = 3.07 \pm 1.03$  was calculated based on the log-normalized organic carbon content-normalized partition coefficient (log  $K_{oc} = 3.6 \text{ L}/\text{kg-oc}$ ) [19] and the organic carbon fraction ( $f_{oc}$ ) [61]:

$$K_d = K_{oc} \cdot f_{oc} / 100 \quad (4)$$

where  $f_{oc} = 0.29 \text{ kg OC}/\text{kg SS}$ , based on the raw SS properties (Table S5).

Multiple data sources [34,6,61,7,92] were used to compile the  $K_d$  for PFAS (see Table S17), either using the  $K_{oc}$  (Eq. 4) or directly obtaining the  $K_d$  values. Missing  $K_d$  values were estimated through the relation log  $K_d$  versus carbon chain length for the different PFAS subgroups (PFCA, PFSA, FTS and PrefOS) (See Fig. S7). The sorption properties of PFAS are related to its fluorocarbon chain length; longer chained such as PFCAs ( $\geq C_7$ ) and PFASAs ( $\geq C_6$ ) are more susceptible to sorb and bioaccumulate in solid fractions than the shorter-chained PFAS ( $\leq C_5$ ), which have higher water-solubility [65].

Regarding HMs, no sorption changes was assumed in de-watering, except for the HMs in the sludge losses from de-watering process (i.e., 5% of SS input mass).

#### 2.3.3. Drying

The average boiling points for BPA is  $361^\circ\text{C}$  and ranging between  $197.2 - 374.0^\circ\text{C}$ , and  $120.2 - 273.2^\circ\text{C}$ , for OPFRs and PFAS, respectively [68,94], so no losses of HOCs are assumed for our drying conditions ( $100^\circ\text{C}$ , 1 atm). The same assumption was considered for HMs.

#### 2.3.4. Anaerobic digestion and pyrolysis

Laboratory analysis data were used to determine the removal rates for HOCs and HMs (values detailed in Table S16), using the samples from the WWTPs and the pyrolysis pilot plant. Samples were collected for the input sludge and the digested sludge in the case of AD, and pyrolyzed sludge (produced from both raw SS and digested sludge). For pyrolysis, a proximate and ultimate analysis of the bio-oil and biochar was done (Table S12), and for gas emission the composition is measured through FTIR (gas composition in Table S10). The product yield of pyrolysis as percentage of biochar, bio-oil and syngas are detailed in

**Table S10.** After pyrolysis, bio-oil and pyrolysis gas are sent to the CHP unit for electricity and heat production, considering process modeling to estimate the energy produced and the associated gaseous emissions (more details in [Table S14](#)).

### 2.3.5. Incineration

Pilot-scale incineration experiments demonstrated the destruction efficiency for OPFRs, which are almost entirely destroyed (>99.999 % destruction efficiency) [57]. Complete removal of BPA was assumed, as no specific data for BPA removal efficiency at our incineration temperature of 850 °C is available. Zhang et al. [93] estimated the influence of operational conditions of incineration on destruction of PFAS, it reported complete mineralization at temperature > 1000 °C; however, a more recent study did show municipal solid waste incineration could release PFAS through the flue gas [9]. Complete destruction of PFAS is thus assumed, although some incomplete fluorinated products could still be emitted [9]. In the case of HMs, a chemical speciation transformation of HMs during incineration process is considered based on literature data [16,52]. The main removal mechanism is volatilization [16] and the HMs residual fraction remains in the solid fraction (ash), except for Cd for which a complete volatilization is considered [65]. The volatilization efficiency of incinerated SS is estimated for As, Cr, Cu, Ni, Pb and Zn ([Table S16](#)). An average volatilization efficiency was assumed (54.7 ± 21 %) for other HMs (Ba, Co, Mo, Sr, and V) for which specific information is missing. Emissions of other pollutants from incineration (e. g., GHGs) are estimated according to the process simulation in Aspen Plus as detail in [Table S14](#).

## 2.4. Climate change and ecotoxicological assessment

### 2.4.1. Life cycle assessment

The different SS treatment scenarios were investigated using LCA by explicitly quantifying inputs of energy and materials and emissions to air, water and soils from each process stage, and estimate the associated environmental impacts for climate change and toxicity effects. Specific removal rates and fate of HOCs and HMs were mapped through different treatment units to identify where emissions or transformations occur, to compare on the effectiveness of each treatment process. The functional unit considered in this study is 1 tonne of SS (i.e., raw SS: wet basis, 75 % moisture) entering the process alternatives. The system boundaries for the case studies are from ‘cradle to grave’, as outlined in [Fig. 2](#). The life cycle inventories for the case studies were estimated by primary data collection from lab experiments and process modelling, complemented with data from the scientific literature through meta-analysis when necessary. These include emission factors, characteristics of waste streams, energy and material balances and information on mass and energy co-products, as summarized in the Supplementary Text 2 and 3. Background life cycle inventories were obtained from Ecoinvent database v3.6, operationalized using Brightway2. Emissions of individual stressors (e.g., CO<sub>2</sub> or CH<sub>4</sub> for climate change and HOCs for human toxicity) were converted to environmental impacts using chemical-specific metrics, also referred as characterization factor (CFs) in LCA [18]. The CFs are simplified measure of the environmental system response to a certain stressor, and are based on physical models of varying complexity linking emissions to impacts [64]. In this study, we assess effects in two impact categories, climate change (at different time horizons) and human and freshwater ecotoxicity.

The SS treatment plant infrastructure is modelled as a wastewater treatment facility with an operational lifespan of 30 years, treating an average annual sewage volume adapted to the processing size in the case study. As in our cases the SS treatment plant does not include the whole WWTP process unit, but only the sludge handling, half of the total plant infrastructure was assumed (made of AD, lime stabilization, dewatering, drying CHP, gas cleaning and biogas upgrading). In the pyrolysis and incineration cases, a synthetic gas factory and waste incineration facility were considered in addition.

In terms of energy recovery, there is none in the baseline cases. In the scenarios with AD, biogas is upgraded and considered as a replacement for natural gas. In the scenarios with pyrolysis, the heat and power from CHP are first used to run the process plant. This requires all the heat, and between 87 % and 54 % of the electric power in C3 scenarios, and between 5.2 % to 7.7 % of it in C4 scenarios (details in [Fig. S8](#)), with the remaining electricity exported to the grid (displacing the average Norwegian power mix). In the incineration cases, both heat and power are produced in surplus, but only the benefits from surplus electricity are considered due to the logistical challenges associated with valorizing the heat.

### 2.4.2. Climate metrics

The climate forcers considered in our study are well-mixed greenhouse gases (WMGHGs), including CO<sub>2</sub>, CH<sub>4</sub> and nitrous oxide (N<sub>2</sub>O), and short-lived climate pollutants (SLCPs), such as NO<sub>x</sub>, CO, SO<sub>x</sub>, NMVOC, organic carbon (OC), and black carbon (BC). The main difference between WMGHGs and SLCPs is their lifetime in the atmosphere. WMGHGs have lifetimes longer than SLCPs (which persist for less than about one year), and while WMGHGs get well mixed in the atmosphere, SLCPs do not [18]. The impact of SLCPs on climate is largely dependent on the emission location, with high concentrations around the emission source, and their effects on climate are most significant in the first few years following the emission [1]. The confidence level in the predicted climate change impacts of SLCPs is lower than WMGHGs, and uncertainty ranges of these characterization factors are considered in the uncertainty analysis. In terms of metrics, one metric representative of short-term effects (GWP20), one of mid-term effects (GWP100, a proxy for changes in global surface temperature about four decades after an emission) [4] and one of long term effects (GTP100) were considered. We refer to other studies for a more extensive definition and discussion of these different metrics [49,84]. For WMGHGs, global average characterization factors from the most recent IPCC report [29] were considered, while for SLCPs characterization factors that are specific for emissions occurring in Europe for GWP20 (for which SLCPs are most relevant) were used, along with global average values for GWP100 and GTP100 [50,64].

### 2.4.3. Ecotoxicological metrics

In LCA, the toxicity impacts of chemicals on human health and freshwaters are typically estimated using characterization factors derived from Usetox™ 2.12, a model endorsed by the UNEP-SETAC Life Cycle Initiative [33,74]. The main output of the database are characterization factors of chemicals, including their fate, exposure, and effect parameters. Usetox™ provides a transparent quantification of human health and ecosystem toxicity CFs for emissions to eight environmental compartments: urban air, continental urban air, household indoor air, industrial indoor air, continental freshwater, continental seawater, continental natural soil and continental agricultural soil [74]. The unit for human toxicity CFs is cumulative cases of either cancer or non-cancer outcomes per kg of pollutant emission (cases/kg<sub>emitted</sub>), and for freshwater ecotoxicity is the potentially affected fraction (PAF) of aquatic species integrated over the exposed water volume (m<sup>3</sup>), time (day) and kg emitted (PAF·m<sup>3</sup>·d//kg<sub>emitted</sub>) [66].

Despite the large number of substances available in the Usetox™ database at the time of this study (3077 organics and 27 inorganics compounds in version 2.12), only twelve OPFRs and three of the analyzed PFAS were present (PFAS CFs not yet included in Usetox™ database). CFs are instead already available for HMs and BPA. In this study, we calculated new CFs for 9 OPFRs and 36 PFAS using the Usetox™ model, whereas other CFs already implemented (12 OPFRs, BPA and 3 PFAS) were updated. The CFs were computed as the result of three main factors: fate factor (FF), exposure factor (XF) and effect factor (EF) [75]. [Tables S18 and S19](#) show the wide range of input parameters that are collected to compute CFs in Usetox™. These data include physico-chemical parameters (e.g., molecular weight, partitioning coefficient

between organic carbon and water, vapor pressure, water solubility, etc.), degradation factors, bioaccumulation, ecotoxicological effects, and carcinogenic and non-carcinogenic effects on human health. The physicochemical parameters provide an estimation of the FF, i.e., mobility of the compounds in water environments, soils and sediments [66]. The XF is defined as the fraction of a substance dissolved in aquatic ecosystems or inhaled or ingested by the human population [26]. The parameters involved in exposure factor calculation are bioaccumulation factors in plant roots, plant leaf, and fish, and biotransfer factors in milk and meat. The EF includes ecotoxicological effects for aquatic environments and human health. The aquatic environment includes freshwater and marine, and the EF is represented by effective concentration affecting 50% of the exposed population (EC50). Since most of the data currently available are for the freshwater environment, this study only considers impacts on freshwater ecotoxicity. For human toxicity, the effective dose affecting 50% of the exposed individuals (ED50) for cancer/non-cancer after inhalation or ingestion is used. In this study, we limit the analysis to ingestion as the only routes of exposure and to non-carcinogenic impacts due to a lack of data on carcinogenic effects of the substances considered, for which studies have been carried out only for three OPFRs (TnBP, TCEP and TDCIPP) and no PFAS. The resulting CFs computed for this analysis are available in Table S20. For each component, the CFs used are specific to the environmental compartment where the toxic components are emitted, i.e. that different toxicity factors are considered if HOCs are directly released to water bodies after de-watering or to agricultural land with the biosolids or the biochar. For emissions to air, we consider emission to urban air; for those to water, emission to continental freshwater; and, for those to soils, emission to continental natural soil. Toxicity impacts are only considered for the

components that are included in the raw SS, so to better highlight the varying effects of the different treatment scenarios.

#### 2.4.4. Statistical and uncertainty analysis

The repercussions of key uncertainties in process parameters and characterization factors on the LCA results was investigated with a Monte Carlo analysis, where 10,000 runs are used to produce results by randomly selecting one value within the uncertainty ranges per each run. Statistical scores are then summarized from these outputs and represented in the results. A range of plausible values are considered for a broad list of parameters related to SS properties, process units, transport distances and characterizations factors, as summarized in Table S21. The ranges considered for elementary composition of raw SS, HMs and HOCs content in raw SS are shown in Table S5 and are based on the standard deviations of the measurements reported by experimental empirical data from our laboratory analysis or from the literature. A triangular probability distribution based on the minimum, maximum and mode of the given range for each parameter is assumed for the selection of the random value, where the mode can be interpreted as the most representative value for the distribution [62].

### 3. Results

#### 3.1. Mapping the fate of HOCs and HMs

Fig. 3 shows the removal rates (degradation) of HOCs and HMs in each scenario, with their fate and remaining concentration in the most relevant output flows (the numerical values are reported in Table S22 and S23). The details of the removal/formation pathway for each

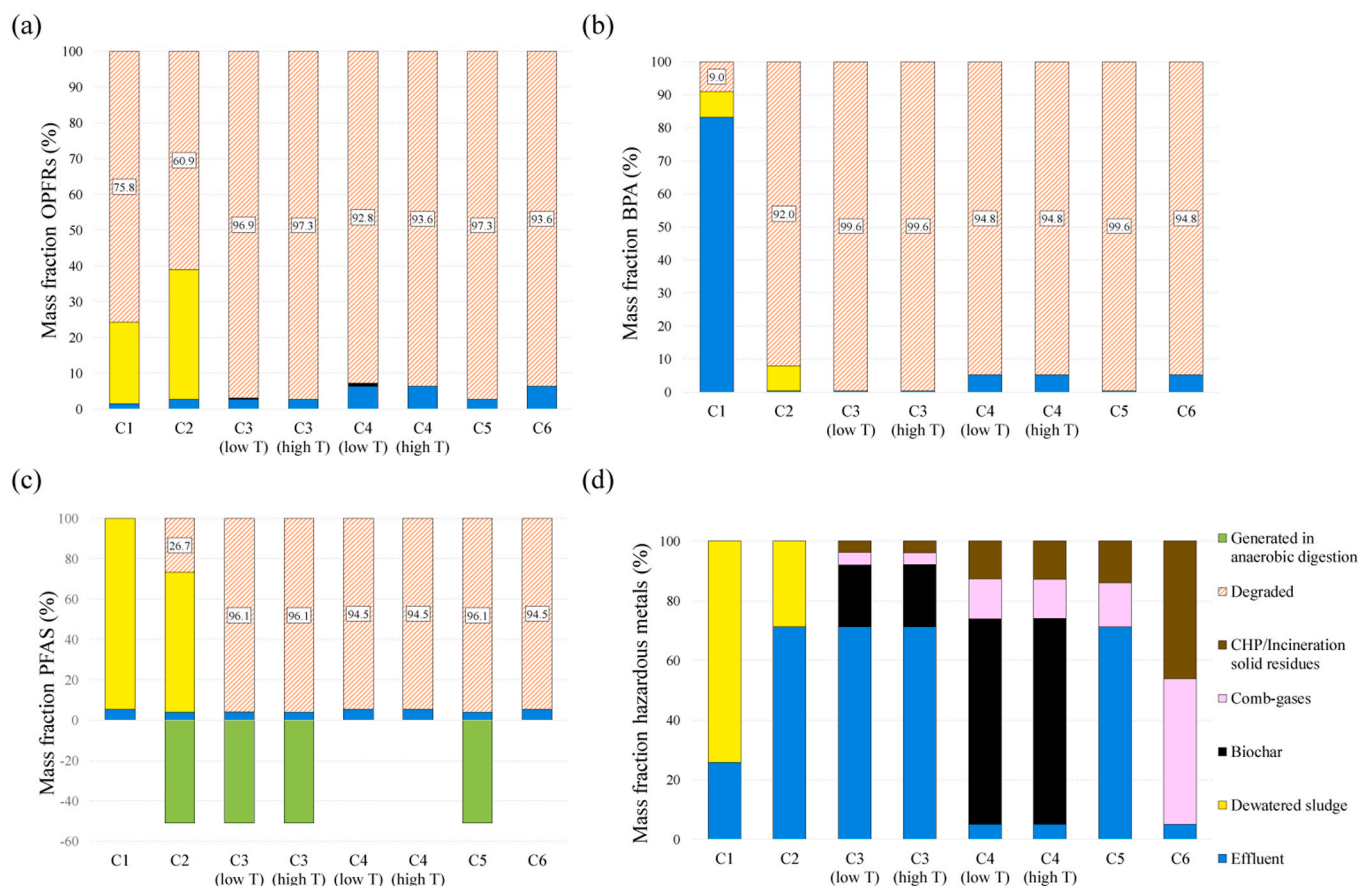


**Fig. 3.** Mass fraction (%) relative to total initial loading (100%) in the raw sewage sludge showing the percentage of degradation and fate of OPFRs (a), BPA (b), PFAs (c) and HMs (d). Effluent indicates liquid emission after de-watering. The results only focus on the direct emissions from the raw sewage sludge treatment pathways and fate of HOCs and HMs in the environment, without considering HOCs emissions of background processes.

pollutant in the different scenarios are available in Figs. S9-S16.

The current dominant SS treatments (C1 and C2) can leave from about 25 % to 40 % of OPFRs undegraded, either flowing to the environment with the wastewaters or left in the dewatered sludge (Fig. 3a). AD has a lower degradation of OPFRs, an aspect that was observed in other studies as well [91]. This is maybe due to OPFRs having a greater chance to volatilize out of the sludge in open systems than closed anaerobic systems [90]. Around 97% of OPFRs are degraded when thermal processes are integrated after AD, i.e., pyrolysis cases (C3 at low and high temperature) and incineration (C5). For thermal processes without AD (C4 and C6), the degradation is around 93 %. The undegraded OPFRs are mainly left in the effluent. The analysis of the specific removal pathways shows that from 36 % to 92 % of total OPFRs are anaerobically digested, except for TEP, 3OH-TBOEP and TTBP for which no degradation is reported (Fig. S10), and the rest mostly remains in the SS. OPFRs left after AD and de-watering are completely degraded when the sludge is pyrolyzed or incinerated (Figs. S11-16). The degradation in conventional treatments (C1 and C2) mainly occurs via hydrolyzation due to lime addition in C1 or during AD in C2. Some alkyl-OPFRs are dominant in the dewatered-sludge, due to a hydrolytic stability to basic pH [82]. TCiPP, TBOEP, TDCiPP and TEHP are the most frequently detected at higher levels in the raw SS (Table S5), and these are almost completely removed after thermal treatments. However, these compounds are also dominant in the output flows of the conventional cases C1 and C2, as they mostly remain in the effluents after de-watering and are thus emitted in the environment.

For BPA (Fig. 3b), the lime addition in the conventional case C1 results in a higher BPA solubility for aqueous solution [53], as the lime can increase the pH of the sludge above the pKa of the bisphenol (ca 10.3), and 83 % of the total BPA is emitted with the effluent. In C2, 92 % of BPA is biodegraded during AD and the rest remains bound to the solid fraction. An almost complete degradation is found in thermal treatments combined with AD (C3 and C5). The thermal pathways without AD (C4 and C6) can achieve a 95 % destruction, while the rest of BPA is left in the effluent after de-watering. The most effective degradation stages are anaerobic digestion (~92 % degradation) and pyrolysis or incineration (complete degradation).

For PFAS, the conventional treatment methods show no (C1) or limited (less than 10 %, C2) degradation, as most of the chemicals remain with the dewatered sludge (Fig. 3c). Biodegradation of PFAS is poorly understood [53], but literature suggests that PFAS are hardly biodegraded due to the fluorine-saturated carbon chain (which is not used as carbon and energy sources by microorganisms [20]) and/or the presence of alkyl chain that discourages the initiation of microbial degradation [71]. The removal rates when thermal treatments are combined to AD are around 96% (C3 and C5), with the remaining PFAS emitted to water bodies. Thermal pathways without AD (C4 and C6) report a PFAS destruction equal to 94.5%, with the remaining PFAS emitted in the effluent (5.5 %).

The analyzed PFAS show a wide range of responses to thermal processes. While they are degraded during pyrolysis and incineration, they can be also generated during AD from precursors [45]. The species formed from precursors are 10:2 FTS, PFOA, PFNA, PFUnDA and PFOS (See Figs. S10, S11, S12 and S15 in SI). PFNA was absent in the input flow to AD, and hence this component is generated from precursors. Other PFAS increase their concentration, such as 10:2 FTS (from  $0.54 \pm 0.16$  to  $0.74$  ng/g-dwSS), PFUnDA (from  $0.29$  to  $112.4 \pm 194.5$  ng/g-dwSS), PFOS (from  $6.86 \pm 7.6$  to  $7.12$  ng/g-dwSS). Previous studies have reported an increase after biological treatments of some stable PFAS, such as PFOS and PFOA, suggesting that biodegradation of precursors such as alcohols and fluorotelomer sulfonates can lead to the formation of these stable PFAS [53]. These newly formed compounds increase the amount of PFAS in the dewatered sludge (and ultimately to soils) if thermal treatments do not follow.

In the conventional treatments, most of PFAS (94.5 % in C1 and 79.6 % in C2) remain in the sludge. In general, the stability of PFAS is

determined by the specific functional group that is attached to the fluoroalkyl tail [93]. PFCAs and PFSAAs are the most stable fluorinated surfactants, in which PFOA (belonging to PFCAs) and PFOS (belonging to PFSAAs) are extremely stable, thermally and chemically, and resistant to both degradation and oxidation [93]. The raw SS is dominated by PFAS-PFCA, specifically by PFOA and PFTrDA.

No HM degradation occurs during the various treatment cases, but their fate as liquid, solid, or airborne emissions can change (Fig. 3d). The addition of AD to the baseline case C1 increases the HMs that are released with the effluents (more than 70 %) and not with the biosolids. The same occurs for the other scenarios that include AD (C3 and C5). Pyrolysis increases the HMs in the biosolids (biochar, in this case), which is particularly high (around 70 %) in the absence of AD, rather than the atmosphere; whereas, combustion releases an increasing quantity of HMs released into the atmosphere (especially Zinc).

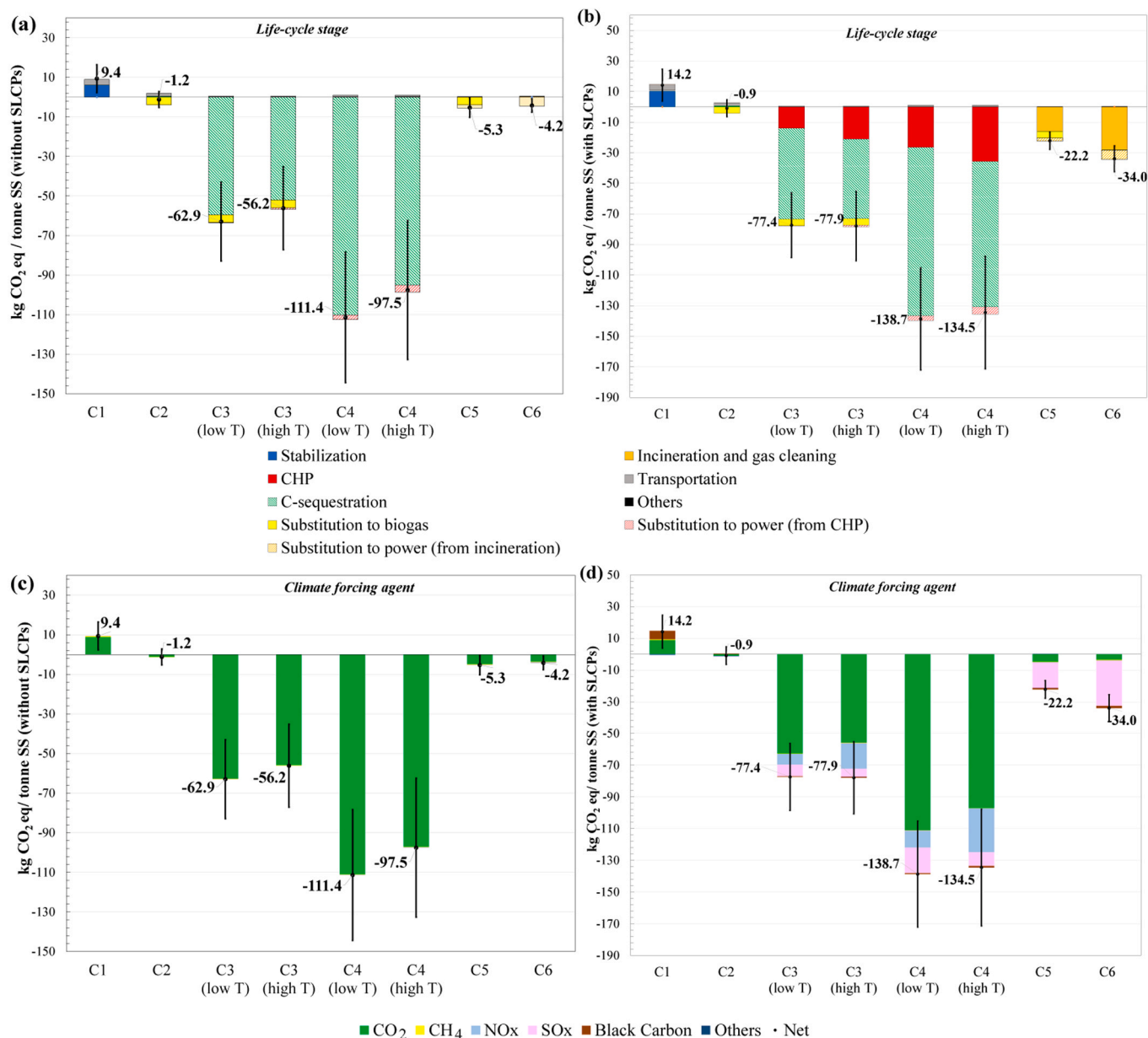
### 3.2. Climate change impacts

Fig. 4 shows climate change impacts (using GWP100) of the scenarios, either without contributions from SLCPs (Fig. 4a, c) or with (Fig. 4b, d), and with a breakdown per main process stage (Fig. 4a, c) or climate forcing agent (Fig. 4b, d).

In general, the baseline scenarios C1 and C2 show higher mean climate impacts than thermal treatments, although the uncertainty ranges can overlap with the incineration-based scenarios. The mean impacts of C1 and C2 are  $9.4$  and  $-1.2$  kg CO<sub>2</sub> eq·tonne<sup>-1</sup> SS, respectively (SLCPs not included). All the thermal treatment scenarios have mean net negative values, which range from about  $-4.2$  to  $-5.3$  kg CO<sub>2</sub> eq·tonne<sup>-1</sup> SS when incineration is involved and from  $-56.2$  to  $-111.4$  kg CO<sub>2</sub> eq·tonne<sup>-1</sup> SS for the pyrolysis-based systems.

The scenarios that include pyrolysis treatment can achieve negative emissions, which is mainly attributable to the long-term carbon storage of biochar in soils. Although it cannot technically be indicated as negative emission, the energy recovery from SS treatment brings additional small climate benefits. As most of the heat produced from CHP and incineration is used by the treatment process itself, the benefits are here related only to the surplus of electricity produced and to biogas (where AD is present). Given the key role played by biochar in climate change mitigation, the more SS is sent to pyrolysis the larger is the resulting climate benefits for the treatment scenario. The exclusion of AD, where some biomass is converted into biogas, ensures that a higher amount of SS is pyrolyzed, and a larger volume of biochar is generated. This is why the negative emissions achieved with C4 are larger than those of C3. Further, the use of a higher temperature during pyrolysis also decreases the quantity of biochar output per unit of SS input, in favor of larger fractions of bio-oil or pyrolytic gas. The cases with pyrolysis undertaken at lower temperatures are thus the ones that achieve larger climate benefits. These findings are generally consistent with other studies that estimated negative climate change impacts for both pyrolysis (ranging from  $-78$  to  $-182$  kg CO<sub>2</sub> eq eq·tonne<sup>-1</sup> SS) and incineration ( $-26$  and  $-131$  kg CO<sub>2</sub> eq eq·tonne<sup>-1</sup> SS) [27]. The main factors for the uncertainty ranges in cases C3 and C4 are the product yield of pyrolysis as percentage of biochar, bio-oil and syngas.

The consideration of the contributions from SLCPs (CO, NO<sub>x</sub>, SO<sub>x</sub>, NMVOC, black carbon and organic carbon), which are typically excluded in previous analysis, can significantly change the overall impacts and increase uncertainty ranges, but the relative ranking of the scenarios remains unaltered (Figs. 4c and 4d). Black carbon is the most important warming species, while the largest cooling effect is induced by NO<sub>x</sub> and SO<sub>x</sub> (mostly released from CHP and incineration). Despite the cooling benefits, these species cause adverse impacts in other impact categories, such as human and ecosystem health or terrestrial acidification [18]. BC also shows relevant warming contributions in the conventional cases, and it is mostly associated with manufacturing. Results generally follow the same pattern when other climate change metrics (GWP20 and GTP100) are considered, as shown in Figs. S17 and S18.



**Fig. 4.** Climate change impacts of raw sewage sludge management scenarios, measured with GWP100. Results are presented by life cycle stage (a, b) and climate forcing agent (c, d). Further, they are presented either without short-lived climate pollutants (SLCPs) (a, c) or with SLCPs (b, d). Black dots represent the mean net GWP100 impacts, and the whiskers show the uncertainty range ( $\pm$  one standard deviation) from the Monte-Carlo analysis. Others in (a, b) include minor contributions from processes like biogas upgrading, pyrolysis, de-watering, soil application, drying and landfill treatment. Others in (c, d) includes climate forcing agents like  $N_2O$ , CO, NMVOC and Organic Carbon.

The impacts are usually higher when a shorter time frame is considered (GWP20), as the importance of  $CH_4$  and SLCPs (when included) is larger. In the longer term (GTP100), the impacts tend to be smaller as the contributions from short-lived species tend to vanish.

### 3.3. Eco-toxicity impacts

The human health toxicity (non-cancerogenic) and freshwater ecotoxicity effects of the investigated SS management scenarios are shown in Fig. 5, in terms of both emissions to environmental compartments and main contributors. Scenarios with higher impacts on human health are those involving incineration, primarily driven by emissions of pollutants to the atmosphere from combustion (Fig. 5a). HMs are the main contributors to human health impacts, in the order  $Zn > Pb > Cd > As > Ba$ , mostly as emissions to air and water bodies. The airborne health effects

of HMs overwhelmed the generally positive effects from abatement of HOCs in the thermal treatment scenarios. C6, which is sending all SS to incineration, has the highest impact, while C3 and C4, where only residuals are used in the CHP unit, the impacts are lower, but still higher than the baseline options not involving treatment units (Fig. 5a). An exception is C4 with pyrolysis occurring at low temperature, where all the contaminants are abated and there are limited emissions of airborne species, since the yields of biochar are higher than in the high temperature case. Air emissions from incineration and pyrolysis account for 28 % to 80 % of impacts for the pyrolysis cases and between 69 % and 95 % for the incineration cases. Note that these emissions could be abated if flue gas cleaning was included in the design of the combustion or pyrolysis process.

After air emissions, the highest contributions to human health are from emissions to water, mostly from the de-watering unit, which range

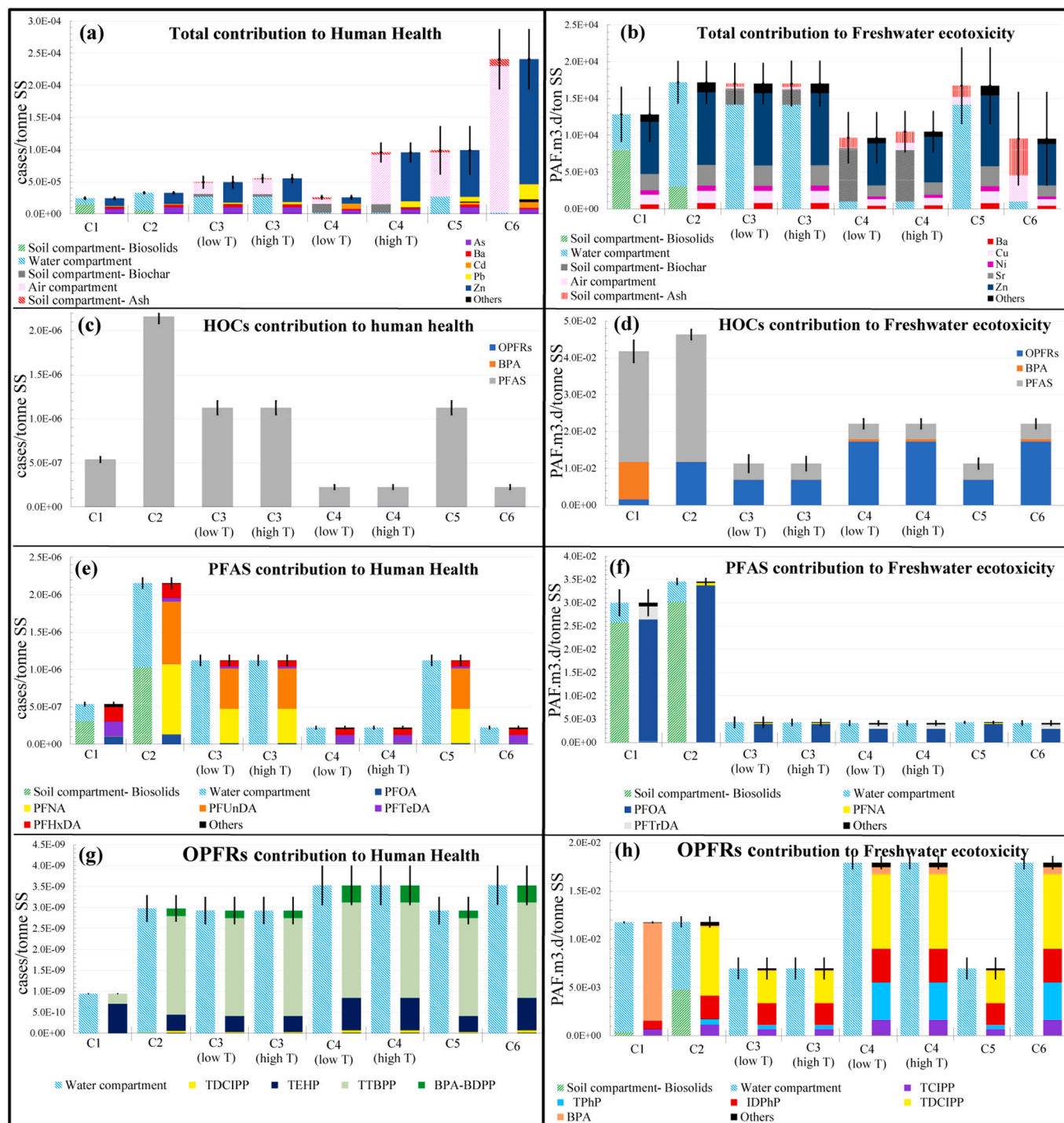


**Fig. 5.** Human (non-cancer effects) and freshwater ecotoxicological impacts of raw sewage sludge management scenarios, with a distinction between impacts to specific environmental compartments and type of pollutant. The results only focus on the direct emissions from the raw sewage sludge treatment pathways and fate of HOCs and HMs in the environment. Total contribution of different emission flows and main compounds to human toxicity potential (a) and freshwater ecotoxicity (b); contribution of HOCs (PFAs, OPFRs, and BPA) to human toxicity (c) and freshwater ecotoxicity (d); focus on the contributions of the main PFAS and emission flows to human toxicity (e) and to freshwater ecotoxicity (f); and contributions of the main OPFRs and emission flows to human toxicity (g) and to freshwater ecotoxicity (h). The ranges indicate the uncertainty (one standard deviation) from the Monte-Carlo analysis, and they are primarily due to the reported ranges in concentrations from laboratory measurements and the characterization of each compound.

from 1 % to 81 % of the total human health impact, and from solid emissions, such as de-watered biosolids (representing 63% of the impact in C1 and 19 % in C2) or biochar (with impacts ranging between 7 % and 8 % in C3 and between 14 % and 53 % in C4).

Regarding freshwater ecotoxicity (Fig. 5b), the inclusion of AD (cases C2, C3 and C5) tends to increase the impacts, while the lowest impacts

occur when all the SS is pyrolyzed or incinerated (C4 and C6). Emissions to the environment via discharge to water and biochar to soil are the main sources of impacts. In general, a large part of the targeted toxic compounds is detected in water emissions after AD in C3 and C5, which are responsible on average of about 82–85 % of the total impacts. In the scenarios without AD, the main contributors to freshwater ecotoxicity

potentials are the emissions with the solids (biosolids, biochar and ash). The pollutants sorbed to solid fractions account for 63 %, 75 %, 67 % and 52 % of the total freshwater ecotoxicity for C1, C4-high T, C4-low T and C6, respectively. Overall, the uncertainty ranges across the freshwater ecotoxicity impacts largely overlap among the various treatment scenarios, preventing from achieving robust conclusions, apart from a clear abatement of freshwater ecotoxicity impacts from HOCs in the thermal treatment cases (Fig. 5d).

HMs are the dominant pollutants affecting human health (>93 % of the impact) and freshwater ecotoxicity potentials (~100 %), with the rest caused by HOCs (Fig. S19). Impacts on human health from HMs are dominated by Zinc (ranging from 38% to 81% of total contributions) and are higher for the scenarios that have a larger volume of sludge or residues combusted, as they increase volatilization of HMs and their dispersal in the environment (Fig. 5a). Zinc also dominates impacts of HMs on freshwater ecotoxicity (Fig. 5b), but to a smaller extent (between 55 % and 59 %) as other species such as Strontium and Copper (up to 17 % of contribution) become more relevant. The ranking of the different scenarios for freshwater ecotoxicity impacts also change relative to human health (Figs. 5a and 5b). In this case, incineration is not the process leading to the highest impacts, but AD as it increases the metals transferred to water bodies. The impacts remain high even when AD is coupled with pyrolysis, and the stand-alone treatment of SS with pyrolysis is the option that causes the smallest potential impacts.

Among the HOCs, impacts on human health are basically only due to emissions of PFAS (Fig. 5c), mostly PFCAs (Fig. 5e). The scenarios with the largest impact are those with AD, especially when it is the main treatment option not associated with other technologies (C2). This is because of the PFAS formed from precursors after AD (i.e., 10:2 FTS, PFOA, PFNA, PFUnDA and PFOS). The complete pyrolysis or incineration of the SS are the most efficient options to abate impacts of PFAS.

PFAS are a main contributor to potential impacts to freshwater ecotoxicity as well in the baseline treatment options (Fig. 5d), but in the scenarios with thermal treatment the effects of PFAS are reduced, making OPFRs (mainly TDCiPP, IDPhP and TPhP) the dominant drivers (Fig. 5h). In this case, scenarios including AD have lower impacts than those without, because of the degradation in AD of some of the main OPFRs present in the SS, i.e., TDCiPP, TPhP and TCiPP, with degradation rates between 67 % and 88.5 % (Table S16). The baseline scenario is also the most inefficient to abate BPA, which has the largest impact to freshwater ecotoxicity across all the assessed scenarios.

The eco-toxicological impacts associated to HOCs are generally related to emissions to water for human health (Fig. 5e for PFAS and 5 g for OPFRs) and to soils for freshwater ecotoxicity impacts (Fig. 5f for PFAS and 5 h for OPFRs). Water emissions of both PFAS and OPFRs strongly affect human health because their CFs associated to water emission is high as shown Fig. 6a and b. However, the concentration change is more of an issue than the increased CFs as the key factor determining the total impact on freshwater ecotoxicity from PFAS (Fig. 5f). For example, even if the CF for freshwater is two times higher for water emissions than soil emissions of PFOA (Fig. 6e), the higher concentration of PFOA released to soil is still the main factor of the high impacts of the conventional cases (C1-C2), in comparison to the impacts of the low emissions to water bodies in thermal treatments (C3-C6).

In general, the potential eco-toxicity impact of a compound is determined by three main factors: concentration, environmental fate and characterization factor. As previously discussed, the thermal treatments do not change the HMs mass flow, but they affect their environmental fate and distribution to environmental compartments (air, soil or water). For example, AD increases the transfer of HMs to water bodies, and pyrolysis and incineration increase the transfer to the atmosphere (the concentration of HMs in the corresponding emission flows are

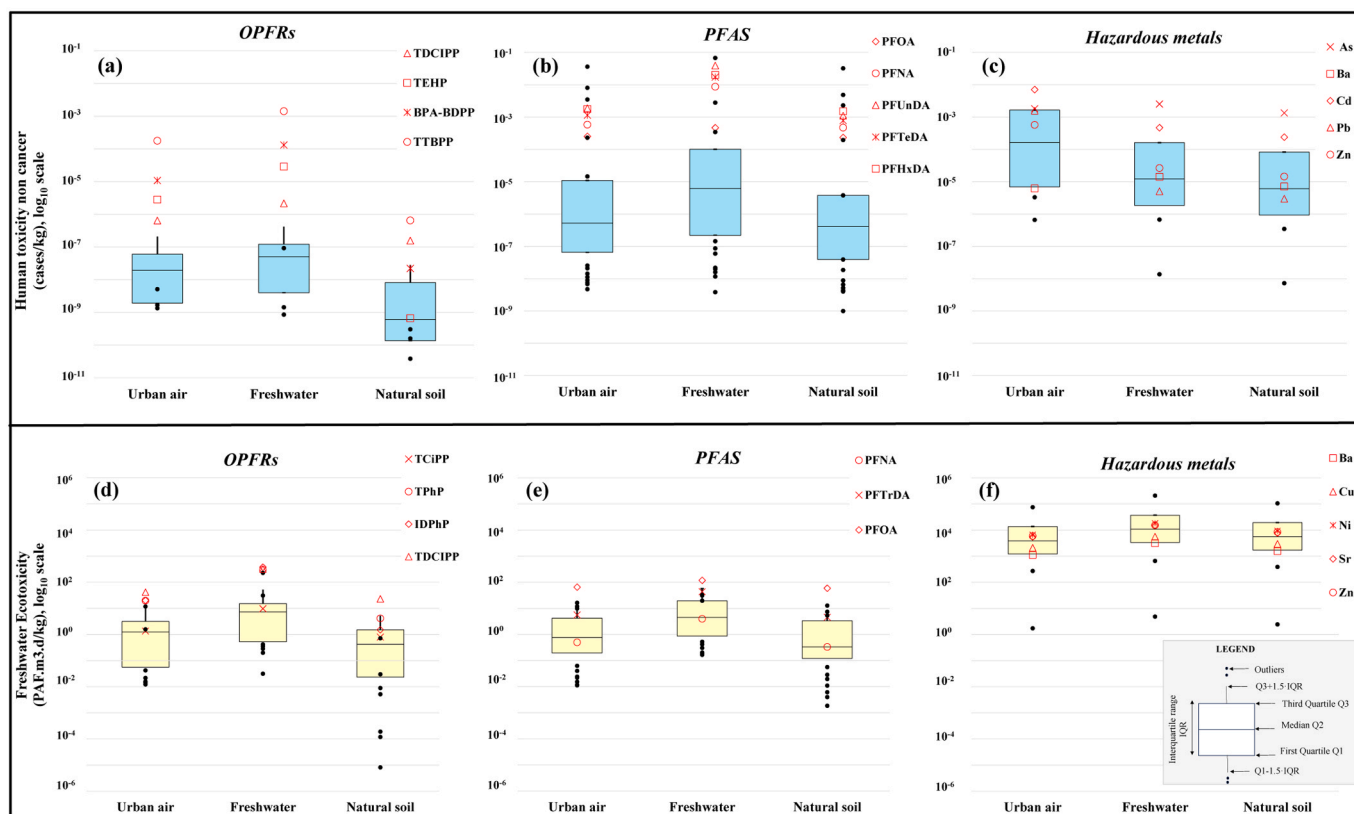


Fig. 6. Boxplots of characterization factors (CFs, shown in log<sub>10</sub> scale) for Human health (cases/kg compound emitted) and Freshwater Ecotoxicity (PAF.m<sup>3</sup>.d/kg compound emitted) for HMs ( $n = 12$ ) and HOCs ( $n = 61$ ) according to the environmental compartments emitted. Note: Red symbols indicate the CFs for the main compounds according to Fig. 5.

detailed in Table S22 and S23). The redistribution of the emission to the environment affects the characterization factors that are used, as different compartments have independent set of values. The median of the effect on human health of HMs emitted to air is about thirteen times higher than median for water (Fig. 6c, logscale), while the median effect on freshwater ecotoxicity of HMs emitted to water bodies is between two and three times higher than the one of emissions to soil and air (Fig. 6f). For the OPFRs and PFAs, characterization factors for both human health and ecotoxicity are higher when these species are released to freshwater (Fig. 6a, b, d, e). The variability in the impact of a same emission into different environmental compartments explains the high toxicological impacts obtained by the thermal treatment options, because HMs emitted to air and water due to pyrolysis/incineration and AD strongly increase human health and freshwater ecotoxicity, respectively. The highest CFs for human health impacts and freshwater ecotoxicity are mainly related to the fate and exposure factors that are combined into the intake fraction matrix, which estimates the fraction of the emission to which the overall population is exposed [74]. For example, airborne emissions of HMs have higher risks of direct exposure through inhalation, while the lower CFs for emissions to other compartments reflect the fact that exposure routes are indirect (e.g., through ingestion of contaminated drinking water, crops, meat, milk and fish) [74].

### 3.4. Energy balances

Thermal treatments (C3 - C6) are energy self-sufficient in terms of heat and power needs (Fig. S8). The heat is provided by the CHP in C3 and C4, and incineration process unit in C5 and C6. Incineration cases are the best for heat production, reporting a surplus of heat produced by the plant, but this is not considered to bring environmental benefits due to logistical challenges of transporting heat. From a power supply point of view, all thermal treatments scenarios report negatives values, i.e., they produce more electricity than what is needed for running the treatment methods. There is a large variation in the net power surplus across the scenarios. For example, AD with pyrolysis at low or high temperature (C3) generate up to 22-times less power than pyrolysis alone (C4). Further, the energy recovery from pyrolysis at high temperature is higher than that at low temperature, as less biochar is produced, and higher quantities of bio-oil and pyrolytic gas can be used for energy production.

## 4. Discussion

Various co-benefits and trade-offs have emerged from the analysis, with some of the new treatment scenarios (C3 and C4 for pyrolysis at high and low temperatures, and C5 and C6 for incineration) able to effectively reduce the HOCs released to the environment while at the same time producing renewable energy and offering opportunities to scale up negative emissions.

This work goes beyond previous studies in several aspects. It compares thermal and non-thermal treatment management for SS by integrating sludge sampling from WWTPs and laboratory analysis of target compounds with detailed process simulations and LCA, so informing about the removal efficiency of each process stage and the associated environmental impacts. It also makes available a wide range of novel characterization factors for PFAs and OPFRs, which can be used in future studies aiming at estimating the toxicity effects of their release in the environment. Different interactions among treatment methods, impacts, and benefits have emerged from the analysis, and are discussed in detail in the following sub-sections.

### 4.1. Energetic benefits

Comparing thermal treatments (C3-C6) with the conventional stabilization treatments (C1 and C2), thermal options have the advantage of producing surplus energy and biochar, which can induce clear

benefits from a multifunctionality and circular economy perspective, with cascading uses of waste products. Thermal treatment provides heat and power from combustion or incineration of bio-oil, pyrolytic gas, or dried sludge. This energy supply in the form of power can bring climate benefits between  $-0.16$  and  $-3.6$  kg CO<sub>2</sub> eq eq-tonne<sup>-1</sup> SS. Heat and power from the incinerator or pyrolysis reactor can be used in other operational units. Larger energy outputs are produced when no AD is included as more biomass is sent to CHP (for combustion) or incineration (C4 and C6) for energy production (Fig. S8). The pyrolysis treatments at high temperature can also produce useful power, which is related to the higher bio-oil yield at higher temperatures (Table S10) that can be converted into energy.

### 4.2. Biochar and negative emissions

Among the thermal treatment options, pyrolysis without anaerobic digestion can produce the larger amounts of biochar and achieve the highest negative emission potential, as it can secure long-term carbon storage by converting the reactive carbon in the sludge into stable biochar carbon [78]. Although thermal treatments can effectively provide heat and power, the main climate change benefits come from the carbon storage capacity of biochar. The biochar stability in soils can last for more than 1000 years, especially when the O:C ratio in the biochar is less than 0.2 [69]. Typically, the O:C ratio decreases as the pyrolysis temperature increases. The biochar obtained at 550 °C and 750 °C has a measured O:C ratio equal to 0.14 and 0.06 (Table S12), respectively, indicating that its stability is longer than 1000 years. Other studies reported the O:C ratio for SS-biochar ranging from 0.45 to 0.11 for temperatures from 500 °C to 900 °C through fast pyrolysis [17], and between 0.12 and 0.01 for temperatures between 500 °C and 700 °C for slow pyrolysis [96]. Overall, the biochar produced from SS is stable once added to soils and can be considered a long-term carbon storage. Biochar also induces changes in soil emissions of N<sub>2</sub>O, NO<sub>x</sub>, CH<sub>4</sub> and other climate forcing agents that are not included in this analysis. Their quantification is highly complex and case/location-specific, as it depends on the biochar type, soil characteristics and environmental conditions [48]. However, changes in soil emissions in the overall GHG balance are relatively small from a life-cycle perspective, as they are less than 2 % of the climate change benefits associated with the long-term carbon storage of biochar [86].

### 4.3. HM concentrations in biochar and dewatered sludge

HMs are major inorganic soil contaminants. The concentration of HMs in sludge and biochar is only one of the parameters to consider when performing ecotoxicological impact assessment, as mobility and bioavailability also play an important role [85]. The long-term stability of HMs in the SS-biochar increases when the biochar is produced at higher temperatures (> 600 °C), while a higher HM leachability is reported for the biochar produced at lower temperatures (< 600 °C) [72]. Generally, a low level of bioavailability and accumulation in plants have been reported for HMs from the SS-biochar [37,60].

Regarding the bioavailability and mobility of HMs from the dewatered SS, a key role is played by the physical and chemical properties of the soil, but also by the neutral/basic pH after lime and anaerobic digestion. HMs are mainly insoluble and immobilized (mainly for Cu, Zn and Cd) [35], while the bioavailability decreased in the order (Cd+Zn) > (Ni+Cu) > (Pb+Cr), i.e., Cd and Zn are generally more available for plants in the soil [69]. According to other studies, the bioavailability can change after lime and AD, e.g., lime stabilization reduces the HMs bioavailability fraction for Cu and Zn [77], while AD increases the bioavailability fraction for Cd and Zn, but reduces for Cu, As, and Pb [95]. In general, field trials based on sludge-derived biochar applied to Norwegian agricultural soils, measuring effects on soil emissions, nutrients, and changes in HM concentrations in soils and edible crops, can better inform about the feasibility and potential risks/benefits of using

biochar produced from dewatered sludge in Norway.

The HMs content in the de-watered SS (C1 and C2) and biochar (C3 and C4) from our investigated scenarios are compared with the limits in the Norwegian and European (EU 2019/1009) regulations [89] for applications as soil improvers in Table S24. The concentration of HMs in both the biochar and dewatered-SS are within the limits defined in the Norwegian (for soil class II) and EU normative for the regulated HMs (As, Cd, Cr, Cu, Pb, Ni and Zn). As the HMs are the key-driver of human health and eco-toxicity impacts, it emphasizes the need for more source control to lower the concentration of HMs in wastewater. A secondary approach would be to ensure that pyrolysis and incineration facilities are developed with appropriate scrubbers to reduce air emissions.

#### 4.4. HOCs concentrations in dewatered sludge and biochar

The levels of emerging contaminants emitted from raw SS from WWTPs (before treatment) range between <LOD and  $8.23 \cdot 10^{-1}$  mg/kg-dwSS for OPFRs, <LOD and  $1.67 \cdot 10^{-1}$  mg/kg-dwSS for PFAS, and  $1.71 \cdot 10^{-1}$  mg/kg-dwSS for BPA (See Table S5). After conventional treatments, the concentration of OPFRs in the dewatered-SS is between 61% and 75% lower than that in the raw SS, with maximum concentrations of  $1.6 \cdot 10^{-1}$  mg/kg-dwSS for C1 and  $4.71 \cdot 10^{-1}$  mg/kg-dwSS for C2. The main OPFR compound in raw, stabilized and dewatered SS is TCiPP (more details in Tables S22 and S23). Pyrolysis significantly reduces the quantity and variety of OPFRs in biochar samples. Biochar produced at low temperatures (500–600 °C) only had measurable quantities of two remaining OPFRs (TBOP at  $2.85 \cdot 10^{-1}$  –  $3.21 \cdot 10^{-1}$  mg/kg-dw biochar and TnBP at  $1.0310^{-3}$  –  $1.84 \cdot 10^{-3}$  mg/kg-dw biochar). Meanwhile, no OPFRs were detected for biochar produced at high temperatures (700–800 °C). No BPA was detected in any biochar produced, but concentrations ranged between  $4.09 \cdot 10^{-3}$  and  $7.3 \cdot 10^{-3}$  mg/kg-dwSS in the dewatered sludge (C1 and C2). As reported above, PFAS are not removed from the dewatered sludge in C1 due to the recalcitrant effect on PFAS of lime addition, and only 18.6 % are removed in the dewatered sludge after AD in C2 (<LOD – 1.05 mg/kg-dwSS). The biochar produced in the different scenarios had non-detectable concentrations (<LOD) of PFAS, except for PFOS (<LOD –  $2.15 \cdot 10^{-4}$  mg/kg-dw biochar).

The use of dewatered-SS or biochar as fertilizer in Norway is regulated by the Regulation no. 951 on fertilizer product of organic origin dated 4th July 2003. Currently, limits are only given for hazardous metals and there are no limits for organic pollutants [10]. The Norwegian normative is only indicating that the material shall not contain "organic pollutants, pesticides, antibiotics/ chemotherapeutics or other manmade organic substances in quantities that can damage public health or the environment when used." At a European level, many countries have introduced stricter limits for selected pollutants [10], but there are no specific considerations of PFAS, BPA or OPFRs.

#### 4.5. Fate of HMs and HOCs during thermal treatments

The main emissions of OPFRs, BPA and PFAS after the stabilization process through lime addition or AD (C1 and C2) occur because these compounds remain attached to the dewatered-SS, except for BPA that is mainly discharged into the water. Although pyrolysis destroys most of the HOCs, some losses are detected in the effluent from the previous dewatering process unit. Pyrolysis coupled to AD fully decomposes BPA. Removal efficiencies are around 100 % for the target OPFRs, in agreement with previous studies that reported a complete decomposition for OPFRs after pyrolysis at temperatures above 500 °C [13]. Removal efficiencies for target PFAS are larger than 94.5 % for pyrolysis and incineration. Removal efficiencies after pyrolysis at  $\geq 500$  °C are almost 100 % for most of the PFAS, except for PFOS that is still detected in the biochar due to its recalcitrant properties. This compound is likely to also be formed by precursors during thermal treatment, of which for PFOS there are many [56]. These results are in agreement with those reported

by Sørmo et al. [83], which shows removal efficiencies above 97 % and 99 % after pyrolysis at temperatures  $\geq 500$  °C and  $\geq 700$  °C, respectively. An important caveat when interpreting this PFAS data is that there may have been other PFAS produced that was not analyzed [3], and further many PFAS and perhaps organophosphate substances may have been formed during thermal treatment that are undetected by the target methods used [79]. In future analysis of OPFR and PFAS destruction technology, it is important to strive for a complete mass balance of phosphate or fluorine, to ensure that there are no unknown, toxic byproducts being formed by the remediation process.

Through anaerobic digestion, most HMs are discharged into the water (C2, C3 and C5), but in the treatment scenarios without AD most of HMs end up into the soil (i.e., dewatered SS for C1, biochar for C4 and ash for C6) and into the atmosphere as air emissions. Overall, pyrolysis increases the HM content of the biochar and incineration produces volatile metallic gaseous emissions, similarly to what reported elsewhere [87]. HMs dominate the toxicity impacts, and their redistribution through the environmental compartments from the alternative treatment options shape their relative performances. For example, while thermal treatments are more efficient to degrade HOCs, their total impact on human health is higher because they volatilize a higher fraction of HMs, thus increasing the risks of being spread in the environment and for human exposure. This is evidenced in the characterization factors for human health associated with hazardous metals emitted to urban air, which are higher than those associated to HMs emitted to water, i.e., indicating a higher ecotoxicological impact of HMs for air than water emissions (Fig. 6c).

Thermal treatments could be optimized to reduce the exposure and risk of HMs, beyond that which was considered in the current study. Factors such as temperature, heating rate, time in the reactor can influence both the volatility and leachability of HMs, as well as the corrosion to the facility [87]. Higher temperature of thermal treatments increase volatilization but decrease leachability in the biochar due to speciation to more stable forms of HM, whereas low temperature treatment does the opposite, indicating a tradeoff with pyrolysis temperature [87]. Some approaches in development, not tested here are adding kaolin or phosphoric acid to reduce volatile emissions [87]. Flue gas cleaning in pyrolysis and incinerations scenarios would reduce the emissions of particles such as HMs and hence reducing the overall ecotoxicological impacts for these scenarios.

#### 4.6. Characterization factor for HOCs

The toxicity of pollutants such as PFAS, BPA and OPFRs require CFs to estimate their human and ecological potential impacts, by accounting for their fate, exposure and effect [66]. There are some studies that apply USEtox to calculate the potential ecotoxicological CFs for pharmaceutical and care products (e.g., Acetaminophen, Amoxicilin, and Lorazepam) [66], textile chemicals [73] and some PFAS (PFOA, PFHxA and PFBS) [36]. However, the CFs for most of the organic chemical pollutants considered in our analysis were still missing. This paper provides new CFs for 21 OPFRs, BPA and 39 PFAS, and transparently reports the data sources used as input parameters to the USEtox model. These values can be used in future studies aiming to assess the toxicity impacts of these compounds. At the same time, some limitations are embedded to these new CFs, such as the exclusion of the terminal degradation products due to a lack of specific data. Long half-lives of HOCs also make it difficult to empirically follow their conversion, and the inclusion of a complex and advanced models to estimate precursor degradation would be required [36]. This example of CFs determination will be helpful to provide a consistent, simple, and transparent way for calculating CFs of other emerging organic pollutants in terms of (eco) toxicity impacts. Further, it should be considered that new research is continuously finding that human health and ecotoxicity impacts for BPA and PFAS are more potent than previously thought [22,23]. Newly available toxicity data could substantially change the CFs in future.

## 5. Conclusions

This study provides a comprehensive investigation of the fate, removal, and toxicological effects of PFAS, OPFRs, BPA and hazardous metals across a range of different treatment management scenarios, together with an estimate of the effects on climate change mitigation and surplus energy supply. Conventional treatments leave about 40 % of OPFRs unabated, and no PFAS are degraded. Pyrolysis and incineration degrade from 94% to 99% of hazardous organic compounds and show a potential to co-deliver negative carbon emissions, while conventional management methods show higher emissions of GHGs. All the thermal treatments considered in the analysis, either with or without anaerobic digestion, are energy self-sufficient and have a surplus of electricity that can be added to the grid mix. The best sludge management options from the point of view of climate change mitigation and reduced eco-toxicity impacts is pyrolysis at low temperature (500–600 °C), without anaerobic digestion. This scenario can produce the highest volumes of biochar for the long-term carbon storage benefits as well as contaminants immobilization and degradation. However, this approach may not solve the risks posed by HMs. These are the dominant pollutants affecting human health (>93 %) and freshwater ecotoxicity potentials (~100 %). HMs are the main contributors to human health impacts through emissions to air, and accounts from 28 % to 80 % of impacts for the pyrolysis cases and between 69% and 95% for the incineration cases. Regarding freshwater ecotoxicity, emissions of HMs to the environment via discharge to water are responsible on average of about 82–85 % of total impacts. Among the HOCs, the impacts on human health are essentially due to emissions of PFAS, with the largest impact in the scenarios considering anaerobic digestion. PFAS are also the main contributor to potential impacts to freshwater ecotoxicity, but in the scenarios with thermal treatment the effects of PFAS are reduced, making OPFRs the dominant drivers.

This analysis also makes available a wide range of novel characterization factors for PFAS and OPFRs, which can be used in future studies aiming at estimating the toxicity effects of their release in the environment. The approach used here where LCA is integrated with laboratory measurements can be reproduced for other pollutants or treatment methods. As these technologies are technically mature, further research should also explore the economic feasibility of the alternative treatment methods in different contexts, and estimate the potential costs and incentives required for a large-scale adoption. Developing these methods for minimization of volatile emissions of HMs, as well as reducing the leaching potential of HMs in the biochar should also be explored. The potential higher costs of the technological shift should not be perceived as a barrier, as it can be mitigated (if not over-compensated) by the benefits from improved human and ecosystem health (in addition to those from reduced climate impacts), with lower expenditures for health care and ecosystem restoration. Such extensive analysis will ultimately support the identification of more holistic win-win solutions for environmental protection and climate change mitigation within a circular economy context.

## Environmental implication

This work compares conventional and thermal treatments of sewage sludge by integrating sludge sampling from wastewater plants of 61 hazardous organic compounds (PFAS and OPFRs) and 12 hazardous metals and laboratory analysis with LCA. It transparently informs about the pollutant removal efficiency of each treatment stage and compares the climate change impacts and toxicity effects to human health and ecosystems of the alternative options. It also makes available a wide range of novel characterization factors for PFAS and OPFRs, which can be used in future studies aiming at estimating the toxicity effects of their release in the environment.

## CRediT authorship contribution statement

**Hans Peter H Arp:** Funding acquisition, Project administration, Supervision, Writing – review & editing. **Gabriela Castro:** Investigation, Writing – review & editing. **Marjorie Morales:** Formal analysis, Investigation, Methodology, Writing – original draft. **Gregory Peters:** Writing – review & editing. **Francesco Cherubini:** Conceptualization, Funding acquisition, Project administration, Supervision, Writing – review & editing. **Alexandros G. Asimakopoulos:** Investigation, Writing – review & editing. **Erlend Sørmo:** Investigation, Writing – review & editing.

## Declaration of Competing Interest

The authors declare that they have no known competing financial interests or personal relationships that could have appeared to influence the work reported in this paper.

## Data Availability

No data was used for the research described in the article.

## Acknowledgements

This study was financially supported by the Norwegian Research Council through the SLUDGEFFECT project (project number: 302371). E.S. acknowledges the support of the VOW project (project number: 299070). Analysis of the organic contaminants was performed at the EnviroChemistry Lab, NTNU.

## Appendix A. Supporting information

Supplementary data associated with this article can be found in the online version at [doi:10.1016/j.jhazmat.2024.134242](https://doi.org/10.1016/j.jhazmat.2024.134242).

## References

- [1] Aamaas, B., Berntsen, T.K., Fuglestedt, J.S., Shine, K.P., Bellouin, N., 2016. Regional emission metrics for short-lived climate forcers from multiple models. *Atmos Chem Phys* 16 (11), 7451–7468. <https://doi.org/10.5194/acp-16-7451-2016>.
- [2] Ahmed, H.K., Fawy, H.A., Abdel-Hady, E., 2010. Study of sewage sludge use in agriculture and its effect on plant and soil. *Agric Biol JN Am* 1 (5), 1044–1049. <https://doi.org/10.5251/abjna.2010.1.5.1044.1049>.
- [3] Alinezhad, A., Challa Sasi, P., Zhang, P., Yao, B., Kubátová, A., Golovko, S.A., et al., 2022. An investigation of thermal air degradation and pyrolysis of per- and polyfluoroalkyl substances and aqueous film-forming foams in soil. *ACS EST Eng* 2 (2), 198–209. <https://doi.org/10.1021/acsesteng.1c00335>.
- [4] Allen, M.R., Fuglestedt, J.S., Shine, K.P., Reisinger, A., Pierrehumbert, R.T., Forster, P.M., 2016. New use of global warming potentials to compare cumulative and short-lived climate pollutants. *Nat Clim Change* 6 (8), 773–776. <https://doi.org/10.1038/nclimate2998>.
- [5] Anderko, L., Pennea, E., 2020. Exposures to per- and polyfluoroalkyl substances (PFAS): potential risks to reproductive and children's health. *Curr Probl Pediatr Adolesc Health Care* 50 (2), 100760. <https://doi.org/10.1016/j.cppeds.2020.100760>.
- [6] Arvaniti, O.S., Andersen, H.R., Thomaidis, N.S., Stasinakis, A.S., 2014. Sorption of perfluorinated compounds onto different types of sewage sludge and assessment of its importance during wastewater treatment. *Chemosphere* 111, 405–411. <https://doi.org/10.1016/j.chemosphere.2014.03.087>.
- [7] Arvaniti, O.S., Ventouri, E.I., Stasinakis, A.S., Thomaidis, N.S., 2012. Occurrence of different classes of perfluorinated compounds in Greek wastewater treatment plants and determination of their solid–water distribution coefficients. *J Hazard Mater* 239 24–31. <https://doi.org/10.1016/j.jhazmat.2012.02.015>.
- [8] Bauer, T., Andreas, L., Lagerkvist, A., Burgman, L.E., 2020. Effects of the different implementation of legislation relating to sewage sludge disposal in the EU. *DETRITUS-Multidiscip J Waste Resour Residues* 10, 92–99. <https://doi.org/10.31025/2611-4135/2020.13944>.
- [9] Björklund, S., Weidemann, E., Jansson, S., 2023. Emission of per- and polyfluoroalkyl substances from a waste-to-energy plant—occurrence in ashes, treated process water, and first observation in flue gas. *Environ Sci Technol* 57 (27), 10089–10095. <https://doi.org/10.1021/acs.est.2c08960>.
- [10] Blytt, L.D., Stang, P., 2018. Organic Pollutants in Norwegian Wastewater Sludge - Results from the Survey in 2017/18 (Norwegian Water Report). *Norsk Vann-Norwegian Water BA, Oslo*, p. 134 (Norwegian Water Report).

- [11] Briffa, J., Sinagra, E., Blundell, R., 2020. Heavy metal pollution in the environment and their toxicological effects on humans. *Heliyon* 6 (9).
- [12] Castro, G., Fourie, A.J., Marlin, D., Venkatraman, V., González, S.V., Asimakopoulos, A.G., 2022. Occurrence of bisphenols and benzophenone UV filters in wild brown mussels (*Perna perna*) from Algoa Bay in South Africa. *Sci Total Environ* 813, 152571. <https://doi.org/10.1016/j.scitotenv.2021.152571>.
- [13] Castro, G., Sormo, E., Yu, G., Sait, S.T., González, S.V., Arp, H.P.H., et al., 2023. Analysis, occurrence and removal efficiencies of organophosphate flame retardants (OPFRs) in sludge undergoing anaerobic digestion followed by diverse thermal treatments. *Sci Total Environ* 870, 161856. <https://doi.org/10.1016/j.scitotenv.2023.161856>.
- [14] Chatziaras, N., Psomopoulos, C.S., Themelis, N.J., 2016. Use of waste derived fuels in cement industry: a review. *Manag Environ Qual: Int J* 27 (2), 178–193. <https://doi.org/10.1108/MEQ-01-2015-0012>.
- [15] Chen, G., Lock Yue, P., Mujumdar, A.S., 2002. Sludge dewatering and drying. *Dry Technol* 20 (4–5), 883–916. <https://doi.org/10.1081/DRT-120003768>.
- [16] Chen, L., Liao, Y., Ma, X., 2019. Heavy metals volatilization characteristics and risk evaluation of co-combusted municipal solid wastes and sewage sludge without and with calcium-based sorbents. *Ecotoxicol Environ Saf* 182, 109370. <https://doi.org/10.1016/j.ecoenv.2019.109370>.
- [17] Chen, T., Zhang, Y., Wang, H., Lu, W., Zhou, Z., Zhang, Y., et al., 2014. Influence of pyrolysis temperature on characteristics and heavy metal adsorptive performance of biochar derived from municipal sewage sludge. *Bioresour Technol* 164, 47–54. <https://doi.org/10.1016/j.biortech.2014.04.048>.
- [18] Cherubini, F., Fuglestedt, J., Gasser, T., Reisinger, A., Cavalett, O., Huijbregts, M. A.J., et al., 2016. Bridging the gap between impact assessment methods and climate science. *Environ Sci Policy* 64, 129–140. <https://doi.org/10.1016/j.envsci.2016.06.019>.
- [19] Choi, Y.J., Lee, L.S., 2017. Partitioning behavior of bisphenol alternatives BPS and BPAF compared to BPA. *Environ Sci Technol* 51 (7), 3725–3732. <https://doi.org/10.1021/acs.est.6b05902>.
- [20] Colosi, L.M., Pinto, R.A., Huang, Q., Weber, W.J.J., 2009. Peroxidase-mediated degradation of perfluorooctanoic acid. *Environ Toxicol Chem: Int J* 28 (2), 264–271. <https://doi.org/10.1897/08-282.1>.
- [21] Di Iaconi, C., Del Moro, G., Bertanza, G., Canato, M., Laera, G., Heimersson, S., et al., 2017. Upgrading small wastewater treatment plants with the sequencing batch biofilter granular reactor technology: Techno-economic and environmental assessment. *J Clean Prod* 148, 606–615. <https://doi.org/10.1016/j.jclepro.2017.02.034>.
- [22] EFSA Panel on Contaminants in the Food Chain, E.C.P., Schrenk, D., Bignami, M., Bodin, L., Chipman, J.K., del Mazo, J., et al., 2020. Risk to human health related to the presence of perfluoroalkyl substances in food. *EFSA J* 18 (9), e06223. <https://doi.org/10.2903/j.efsa.2020.6223>.
- [23] EFSA Panel on Food Contact Materials, E.A.P.A.C., Lambré, C., Barat Baviera, J.M., Bolognesi, C., Chesson, A., Cocconcelli, P.S., et al., 2023. Re-evaluation of the risks to public health related to the presence of bisphenol A (BPA) in foodstuffs. *EFSA J* 21 (4), e06857. <https://doi.org/10.2903/j.efsa.2023.6857>.
- [24] Eurostat, 2021. Urban Waste Water Treatment in Europe. Statistical Office of the European Union, European Environment Agency.
- [25] Eurostat, 2023. Sewage sludge production and disposal. ([https://ec.europa.eu/eurostat/databrowser/view/env\\_ww\\_spd/default/table?lang=en](https://ec.europa.eu/eurostat/databrowser/view/env_ww_spd/default/table?lang=en)).
- [26] Fantke, P.E., Bijster, M., Guignard, C., Hauschild, M., Huijbregts, M., Jolliet, O., et al., 2017. USEtox® 2.0 Documentation (Version 1.1). Technical University of Denmark, p. 208.
- [27] Faragó, M., Damgaard, A., Logar, I., Rygaard, M., 2022. Life cycle assessment and cost-benefit analysis of technologies in water resource recovery facilities: the case of sludge pyrolysis. *Environ Sci Technol* 56 (24), 17988–17997. <https://doi.org/10.1021/acs.est.2c06083>.
- [28] Fernando-Foncellas, C., Estevez, M.M., Uellendahl, H., Varrone, C., 2021. Co-management of sewage sludge and other organic wastes: a Scandinavian case study. *Energies* 14 (12), 3411. <https://doi.org/10.3390/en14123411>.
- [29] Forster, P., Storelvmo, T., Armour, K., Collins, W., Dufresne, J.-L., Frame, D., et al., 2021. The Earth's energy budget, climate feedbacks, and climate sensitivity. In: Masson-Delmotte, V., Zhai, P., Pirani, A., Connors, S.L., Péan, C., Berger, S., Caud, N., Chen, Y., Goldfarb, L., Gomis, M.I., Huang, M., Leitzell, K., Lonnoy, E., Matthews, J.B.R., Maycock, T.K., Waterfield, T., Yelekçi, O., Yu, R., Zhou, B. (Eds.), *Climate Change 2021: The Physical Science Basis. Contribution of Working Group I to the Sixth Assessment Report of the Intergovernmental Panel on Climate Change*. Cambridge University Press, United Kingdom and New York, NY, USA, pp. 923–1054. <https://doi.org/10.1017/9781009157896>.
- [30] Fu, Q., Wang, D., Li, X., Yang, Q., Xu, Q., Ni, B.-J., et al., 2021. Towards hydrogen production from waste activated sludge: principles, challenges and perspectives. *Renew Sustain Energy Rev* 135, 110283. <https://doi.org/10.1016/j.rser.2020.110283>.
- [31] Goyal, D., Yadav, A., Prasad, M., Singh, T.B., Shrivastav, P., Ali, A., et al., 2020. Effect of Heavy Metals on Plant Growth: An Overview. In: Naeem, M., Ansari, A.A., Gill, S.S. (Eds.), *Contaminants in Agriculture: Sources, Impacts and Management*. Springer International Publishing, Cham, pp. 79–101. [https://doi.org/10.1007/978-3-030-41552-5\\_4](https://doi.org/10.1007/978-3-030-41552-5_4).
- [32] Havukainen, J., Saud, A., Astrup, T.F., Peltola, P., Hortalainen, M., 2022. Environmental performance of dewatered sewage sludge digestate utilization based on life cycle assessment. *Waste Manag* 137, 210–221. <https://doi.org/10.1016/j.wasman.2021.11.005>.
- [33] Henderson, A.D., Hauschild, M.Z., van de Meent, D., Huijbregts, M.A.J., Larsen, H. F., Margni, M., et al., 2011. USEtox fate and ecotoxicity factors for comparative assessment of toxic emissions in life cycle analysis: sensitivity to key chemical properties. *Int J Life Cycle Assess* 16 (8), 701–709. <https://doi.org/10.1007/s11367-011-0294-6>.
- [34] Higgins, C.P., Luthy, R.G., 2006. Sorption of perfluorinated surfactants on sediments. *Environ Sci Technol* 40 (23), 7251–7256. <https://doi.org/10.1021/es061000n>.
- [35] Hoang, S.A., Bolan, N., Madhubashani, A., Vithanage, M., Perera, V., Wijesekara, H., et al., 2022. Treatment processes to eliminate potential environmental hazards and restore agronomic value of sewage sludge: a review. *Environ Pollut* 293, 118564. <https://doi.org/10.1016/j.envpol.2021.118564>.
- [36] Holmquist, H., Fantke, P., Cousins, I.T., Owsianiak, M., Liagkouridis, I., Peters, G. M., 2020. An (Eco)toxicity life cycle impact assessment framework for per- and polyfluoroalkyl substances. *Environ Sci Technol* 54 (10), 6224–6234. <https://doi.org/10.1021/acs.est.9b07774>.
- [37] Hossain, M.K., Strezov, V., Chan, K.Y., Nelson, P.F., 2010. Agronomic properties of wastewater sludge biochar and bioavailability of metals in production of cherry tomato (*Lycopersicon esculentum*). *Chemosphere* 78 (9), 1167–1171. <https://doi.org/10.1016/j.chemosphere.2010.01.009>.
- [38] Hsiao, P.C., Lo, S.L., 1997. Effects of lime treatment on fractionation and extractabilities of heavy metals in sewage sludge. *J Environ Sci Health Part A* 32 (9–10), 2521–2536. <https://doi.org/10.1080/10934529709376700>.
- [39] Huang, C., Mohamed, B.A., Li, L.Y., 2022. Comparative life-cycle assessment of pyrolysis processes for producing bio-oil, biochar, and activated carbon from sewage sludge. *Resour Conserv Recycl* 181, 106273. <https://doi.org/10.1016/j.resconrec.2022.106273>.
- [40] Hudcová, H., Vymazal, J., Rozkošný, M., 2019. Present restrictions of sewage sludge application in agriculture within the European Union. *Soil Water Res* 14 (2), 104–120. <https://doi.org/10.17221/36/2018-SWR>.
- [41] Ivashchkin, P., Corvini, P.-X., Dohmann, M., 2004. Behaviour of endocrine disrupting chemicals during the treatment of municipal sewage sludge. *Water Sci Technol* 50 (5), 133–140. <https://doi.org/10.2166/wst.2004.0320>.
- [42] Kelessidis, A., Stasinakis, A.S., 2012. Comparative study of the methods used for treatment and final disposal of sewage sludge in European countries. *Waste Manag* 32 (6), 1186–1195. <https://doi.org/10.1016/j.wasman.2012.01.012>.
- [43] Krahn, K.M., Cornelissen, G., Castro, G., Arp, H.P.H., Asimakopoulos, A.G., Wolf, R., et al., 2023. Sewage sludge biochars as effective PFAS-sorbents. *J Hazard Mater* 445, 130449. <https://doi.org/10.1016/j.jhazmat.2022.130449>.
- [44] Kwapiński, W., Kolinovic, I., Leahy, J.J., 2021. Sewage sludge thermal treatment technologies with a focus on phosphorus recovery: a review. *Waste Biomass-Valoriz* 12 (11), 5837–5852. <https://doi.org/10.1007/s12649-020-01280-2>.
- [45] Lakshminarasimman, N., Gewurtz, S.B., Parker, W.J., Smyth, S.A., 2021. Removal and formation of perfluoroalkyl substances in Canadian sludge treatment systems – a mass balance approach. *Sci Total Environ* 754, 142431. <https://doi.org/10.1016/j.scitotenv.2020.142431>.
- [46] Lam, C.H., Ip, A.W., Barford, J.P., McKay, G., 2010. Use of incineration MSW ash: a review. *Sustainability* 2 (7), 1943–1968. <https://doi.org/10.3390/su2071943>.
- [47] LeBlanc, R.J., Matthews, P., Richard, R.P., 2009. *Global Atlas of Excreta, Wastewater Sludge, and Biosolids Management: Moving Forward the Sustainable and Welcome Uses of A Global Resource*. Un-habitat.
- [48] Lehmann, J., Cowie, A., Masiello, C.A., Kammann, C., Woolf, D., Amonette, J.E., et al., 2021. Biochar in climate change mitigation. *Nat Geosci* 14 (12), 883–892. <https://doi.org/10.1038/s41561-021-00852-8>.
- [49] Levasseur, A., Cavalett, O., Fuglestedt, J.S., Gasser, T., Johansson, D.J., Jørgensen, S.V., et al., 2016. Enhancing life cycle impact assessment from climate science: Review of recent findings and recommendations for application to LCA. *Ecol Indic* 71, 163–174. <https://doi.org/10.1016/j.ecolind.2016.06.049>.
- [50] Levasseur, A., de Schryver, A., Hauschild, M., Kabe, Y., Sahnoune, A., Tanaka, K., et al., 2016. Greenhouse gas emissions and climate change impacts. In: Frischknecht, R., Jolliet, O. (Eds.), *Global Guidance for Life Cycle Impact Assessment Indicators*. UNEP/SETAC Life Cycle Initiative, pp. 58–75.
- [51] Liang, K., Liu, J., 2016. Understanding the distribution, degradation and fate of organophosphate esters in an advanced municipal sewage treatment plant based on mass flow and mass balance analysis. *Sci Total Environ* 544, 262–270. <https://doi.org/10.1016/j.scitotenv.2015.11.112>.
- [52] Liu, Z., Qian, G., Sun, Y., Xu, R., Zhou, J., Xu, Y., 2010. Speciation evolutions of heavy metals during the sewage sludge incineration in a laboratory scale incinerator. *Energy Fuels* 24 (4), 2470–2478. <https://doi.org/10.1021/ef901060u>.
- [53] Mahinroosta, R., Senevirathna, L., 2020. A review of the emerging treatment technologies for PFAS contaminated soils. *J Environ Manag* 255, 109896. <https://doi.org/10.1016/j.jenvman.2019.109896>.
- [54] Mannarino, G., Caffaz, S., Gori, R., Lombardi, L., 2022. Environmental life cycle assessment of hydrothermal carbonization of sewage sludge and its products valorization pathways. *Waste Biomass-Valoriz* 13 (9), 3845–3864. <https://doi.org/10.1007/s12649-022-01821-x>.
- [55] Margot, J., Rossi, L., Barry, D.A., Holliger, C., 2015. A review of the fate of micropollutants in wastewater treatment plants. *WIREs Water* 2 (5), 457–487. <https://doi.org/10.1002/wat2.1090>.
- [56] Martin, J.W., Asher, B.J., Beeson, S., Benskin, J.P., Ross, M.S., 2010. PFOS or PreFOS? Are perfluorooctane sulfonate precursors (PreFOS) important determinants of human and environmental perfluorooctane sulfonate (PFOS) exposure? *J Environ Monit* 12 (11), 1979–2004. <https://doi.org/10.1039/COEM00295J>.
- [57] Matsukami, H., Kose, T., Watanabe, M., Takigami, H., 2014. Pilot-scale incineration of wastes with high content of chlorinated and non-halogenated organophosphorus flame retardants used as alternatives for PBDEs. *Sci Total Environ* 493, 672–681. <https://doi.org/10.1016/j.scitotenv.2014.06.062>.

- [58] Mayer, F., Bhandari, R., Gäth, S.A., 2021. Life cycle assessment of prospective sewage sludge treatment paths in Germany. *J Environ Manag* 290, 112557. <https://doi.org/10.1016/j.jenvman.2021.112557>.
- [59] Medina-Martos, E., Istrate, I.-R., Villamil, J.A., Gálvez-Martos, J.-L., Dufour, J., Mohedano, Á.F., 2020. Techno-economic and life cycle assessment of an integrated hydrothermal carbonization system for sewage sludge. *J Clean Prod* 277, 122930. <https://doi.org/10.1016/j.jclepro.2020.122930>.
- [60] Mendez, A., Gomez, A., Paz-Ferreiro, J., Gasco, G., 2012. Effects of sewage sludge biochar on plant metal availability after application to a Mediterranean soil. *Chemosphere* 89 (11), 1354–1359. <https://doi.org/10.1016/j.chemosphere.2012.05.092>.
- [61] Meng, L., Song, B., Zhong, H., Ma, X., Wang, Y., Ma, D., et al., 2021. Legacy and emerging per-and polyfluoroalkyl substances (PFAS) in the Bohai Sea and its inflow rivers. *Environ Int* 156, 106735. <https://doi.org/10.1016/j.envint.2021.106735>.
- [62] Muller, S., Mutel, C., Lesage, P., Samson, R., 2018. Effects of distribution choice on the modeling of life cycle inventory uncertainty: an assessment on the ecoinvent v2.2 database. *J Ind Ecol* 22 (2), 300–313. <https://doi.org/10.1111/jiec.12574>.
- [63] Murakami, T., Suzuki, Y., Nagasawa, H., Yamamoto, T., Koseki, T., Hirose, H., et al., 2009. Combustion characteristics of sewage sludge in an incineration plant for energy recovery. *Fuel Process Technol* 90 (6), 778–783. <https://doi.org/10.1016/j.fuproc.2009.03.003>.
- [64] Myhre, G., Shindell, D., Pongratz, J., 2013. Anthropogenic and natural radiative forcing. In: Stocker, T., Qin, D., Plattner, G.-K., Tignor, M., Allen, S., Boschung, J., Nauels, A., Xia, Y., Bex, V., Midgley, P. (Eds.), *Climate Change 2013: The Physical Science Basis. Working Group I Contribution to the Fifth Assessment Report of the Intergovernmental Panel on Climate Change*. Cambridge University Press, United Kingdom and New York, USA, pp. 659–740.
- [65] Olsson, A., 2016. Local Pollution and the Risks of OPFR, PBDE and PFAS to the Marine Ecosystem Outside Longyearbyen and Barentsburg in Svalbard. *Aquat. Ecol. Lunds Universitet, Lund*.
- [66] Ortiz de García, S., García-Encina, P.A., Irusta-Mata, R., 2017. The potential ecotoxicological impact of pharmaceutical and personal care products on humans and freshwater, based on USEtox™ characterization factors. A Spanish case study of toxicity impact scores. *Sci Total Environ* 609, 429–445. <https://doi.org/10.1016/j.scitotenv.2017.07.148>.
- [67] Panieri, E., Baralic, K., Djukic-Cosic, D., Buha Djordjevic, A., Saso, L., 2022. PFAS molecules: a major concern for the human health and the environment. *Toxics* 10 (2), 44. <https://doi.org/10.3390/toxics10020044>.
- [68] PubChem-database, 2023. Compound Summary. US National Institutes of Health (NIH). National Center for Biotechnology Information. (<https://pubchem.ncbi.nlm.nih.gov>).
- [69] Racek, J., Sevcik, J., Chorazy, T., Kucerik, J., Hlavinec, P., 2020. Biochar – recovery material from pyrolysis of sewage sludge: a review. *Waste Biomass-Valoriz* 11 (7), 3677–3709. <https://doi.org/10.1007/s12649-019-00679-w>.
- [70] Rangabhushiyam, S., Lins, P.Vd.S., Oliveira, L.M.Td.M., Sepulveda, P., Ighalo, J.O., Rajapaksha, A.U., et al., 2022. Sewage sludge-derived biochar for the adsorptive removal of wastewater pollutants: a critical review. *Environ Pollut* 293, 118581. <https://doi.org/10.1016/j.envpol.2021.118581>.
- [71] Rayne, S., Forest, K., 2009. Perfluoroalkyl sulfonic and carboxylic acids: a critical review of physicochemical properties, levels and patterns in waters and wastewaters, and treatment methods. *J Environ Sci Health Part A* 44 (12), 1145–1199. <https://doi.org/10.1080/10934520903139811>.
- [72] Roberts, D.A., Cole, A.J., Whelan, A., de Nys, R., Paul, N.A., 2017. Slow pyrolysis enhances the recovery and reuse of phosphorus and reduces metal leaching from biosolids. *Waste Manag* 64, 133–139. <https://doi.org/10.1016/j.wasman.2017.03.012>.
- [73] Roos, S., Holmquist, H., Jönsson, C., Arvidsson, R., 2018. USEtox characterisation factors for textile chemicals based on a transparent data source selection strategy. *Int J Life Cycle Assess* 23, 890–903. <https://doi.org/10.1007/s11367-017-1330-y>.
- [74] Rosenbaum, R.K., Bachmann, T.M., Gold, L.S., Huijbregts, M.A.J., Jolliet, O., Juraske, R., et al., 2008. USEtox—the UNEP-SETAC toxicity model: recommended characterisation factors for human toxicity and freshwater ecotoxicity in life cycle impact assessment. *Int J Life Cycle Assess* 13 (7), 532–546. <https://doi.org/10.1007/s11367-008-0038-4>.
- [75] Rosenbaum, R.K., Margni, M., Jolliet, O., 2007. A flexible matrix algebra framework for the multimedia multipathway modeling of emission to impacts. *Environ Int* 33 (5), 624–634. <https://doi.org/10.1016/j.envint.2007.01.004>.
- [76] Samaras, P., Papadimitriou, C., Haritou, I., Zouboulis, A., 2008. Investigation of sewage sludge stabilization potential by the addition of fly ash and lime. *J Hazard Mater* 154 (1-3), 1052–1059. <https://doi.org/10.1016/j.jhazmat.2007.11.012>.
- [77] Shaheen, S.M., Shams, M.S., Ibrahim, S.M., Elbehiry, F.A., Antoniadis, V., Hooda, P.S., 2014. Stabilization of sewage sludge by using various by-products: effects on soil properties, biomass production, and bioavailability of copper and zinc. *Water Air Soil Pollut* 225 (7), 2014. <https://doi.org/10.1007/s11270-014-2014-x>.
- [78] Singh, S., Kumar, V., Dhanjal, D.S., Datta, S., Bhatia, D., Dhiman, J., et al., 2020. A sustainable paradigm of sewage sludge biochar: valorization, opportunities, challenges and future prospects. *J Clean Prod* 269, 122259. <https://doi.org/10.1016/j.jclepro.2020.122259>.
- [79] Smith, S.J., Lauria, M., Higgins, C.P., Pennell, K.D., Blotvogel, J., Arp, H.P.H., 2024. The need to include a fluorine mass balance in the development of effective technologies for PFAS destruction. *Environ Sci Technol* 58 (6), 2587–2590. <https://doi.org/10.1021/acs.est.3c10617>.
- [80] SSB, 2021. Sewage Sludge, by Category of Disposal, Contents and Year, 13.10.2022 ed. Statistics Norway, Statistikkbanken.
- [81] SSB, 2021. Sewage Sludge, by Contents and Year, 13.10.2022 ed. Statistics Norway, Statistikkbanken.
- [82] Su, G., Letcher, R.J., Yu, H., 2016. Organophosphate flame retardants and plasticizers in aqueous solution: pH-dependent hydrolysis, kinetics, and pathways. *Environ Sci Technol* 50 (15), 8103–8111. <https://doi.org/10.1021/acs.est.6b02187>.
- [83] Sormo, E., Castro, G., Hubert, M., Licul-Kucera, V., Quintanilla, M., Asimakopoulos, A.G., et al., 2023. The decomposition and emission factors of a wide range of PFAS in diverse, contaminated organic waste fractions undergoing dry pyrolysis. *J Hazard Mater* 454, 131447. <https://doi.org/10.1016/j.jhazmat.2023.131447>.
- [84] Tanaka, K., Cavaletto, O., Collins, W.J., Cherubini, F., 2019. Asserting the climate benefits of the coal-to-gas shift across temporal and spatial scales. *Nat Clim Change* 9 (5), 389–396. <https://doi.org/10.1038/s41558-019-0457-1>.
- [85] Tarpani, R.R.Z., Alfonsin, C., Hospido, A., Azapagic, A., 2020. Life cycle environmental impacts of sewage sludge treatment methods for resource recovery considering ecotoxicity of heavy metals and pharmaceutical and personal care products. *J Environ Manag* 260, 109643. <https://doi.org/10.1016/j.jenvman.2019.109643>.
- [86] Tisserant, A., Morales, M., Cavaletto, O., O'Toole, A., Weldon, S., Rasse, D.P., et al., 2022. Life-cycle assessment to unravel co-benefits and trade-offs of large-scale biochar deployment in Norwegian agriculture. *Resour. Conserv Recycl* 179, 106030. <https://doi.org/10.1016/j.resconrec.2021.106030>.
- [87] Udayanga, W.C., Veksha, A., Giannis, A., Lisak, G., Chang, V.W.-C., Lim, T.-T., 2018. Fate and distribution of heavy metals during thermal processing of sewage sludge. *Fuel* 226, 721–744. <https://doi.org/10.1016/j.fuel.2018.04.045>.
- [88] Vierke, L., Berger, U., Cousins, I.T., 2013. Estimation of the acid dissociation constant of perfluoroalkyl carboxylic acids through an experimental investigation of their water-to-air transport. *Environ Sci Technol* 47 (19), 11032–11039. <https://doi.org/10.1021/es402691z>.
- [89] VKM, Eggen, T., Amlund, H., Barnevelde, R., Bernhoft, A., Bloem, E., et al., 2022. Risk assessment of potentially toxic elements (heavy metals and arsenic) in soil and fertiliser products – fate and effects in the food chain and the environment in Norway. Norwegian Scientific Committee for Food and Environment (VKM), Oslo, Norway.
- [90] Wang, S., Wen, Y., Shi, Z., Nuran Zaini, I., Göran Jönsson, P., Yang, W., 2022. Novel carbon-negative methane production via integrating anaerobic digestion and pyrolysis of organic fraction of municipal solid waste. *Energy Convers Manag* 252, 115042. <https://doi.org/10.1016/j.enconman.2021.115042>.
- [91] Yang, X., Fan, D., Gu, W., Liu, J., Shi, L., Zhang, Z., et al., 2021. Aerobic and anaerobic biodegradability of organophosphates in activated sludge derived from kitchen garbage biomass and agricultural residues. *Front Bioeng Biotechnol* 9. <https://doi.org/10.3389/fbioe.2021.649049>.
- [92] Zhang, C., Yan, H., Li, F., Hu, X., Zhou, Q., 2013. Sorption of short-and long-chain perfluoroalkyl surfactants on sewage sludges. *J Hazard Mater* 260, 689–699. <https://doi.org/10.1016/j.jhazmat.2013.06.022>.
- [93] Zhang, J., Gao, L., Bergmann, D., Bulatovic, T., Surapaneni, A., Gray, S., 2023. Review of influence of critical operation conditions on by-product/intermediate formation during thermal destruction of PFAS in solid/biosolids. *Sci Total Environ* 854, 158796. <https://doi.org/10.1016/j.scitotenv.2022.158796>.
- [94] Zhang, M., Suuberg, E.M., 2023. Estimation of vapor pressures of perfluoroalkyl substances (PFAS) using COSMOtherm. *J Hazard Mater* 443, 130185. <https://doi.org/10.1016/j.jhazmat.2022.130185>.
- [95] Zheng, X., Zou, D., Wu, Q., Wang, H., Li, S., Liu, F., et al., 2022. Review on fate and bioavailability of heavy metals during anaerobic digestion and composting of animal manure. *Waste Manag* 150, 75–89. <https://doi.org/10.1016/j.wasman.2022.06.033>.
- [96] Zielińska, A., Oleszczuk, P., Charnas, B., Skubiszewska-Zięba, J., Pasieczna-Patkowska, S., 2015. Effect of sewage sludge properties on the biochar characteristic. *J Anal Appl Pyrolysis* 112, 201–213. <https://doi.org/10.1016/j.jaap.2015.01.025>.